

BABAR MUON DETECTOR UPGRADE

Sanjay Kumar Swain

Stanford Linear Accelerator Center

- **Introduction**
- **RPC → LST**
- **Detector components**
- **Installation**
- **Performance**
- **Conclusion**



BABAR LST Team

M. Andreotti, D. Bettoni, R. Calabrese, V. Carassiti,
G. Cibinetto, A. Cotta Ramusino, M. Negrini, L. Piemontese, V. Santoro
Ferrara University and INFN
P. Patteri

Laboratori Nazionali di Frascati dell'INFN

R. Capra, M. Lo Vetere, S. Minutoli, P. Musico, E. Robutti, S. Tosi
Genova University and INFN

C. Simani, D. Lange, C-S Cheng
Livermore National Laboratory

Y. Zheng
MIT

T. Allmendinger, G. Benelli, M. Gee, L. Corwin, K.Honscheid, R. Kass, R. King, J. Regensburger,
C. Rush, S. Smith, Q. Wong
Ohio State University

C. Fanin, M. Morandin, M. Posocco, M. Rotondo, R. Stroili
Padova University and INFN

R. Covarelli
Perugia
W. Menges

Queen Mary, University of London

J. Biesiada, G-L. Cavoto, N. Danielson, R. Fernholz, Y. Lau, C. Lu, J. Olsen, W. Sands, A.J.S. Smith, A. Telnov
Princeton University

B. Fulsom

University of British Columbia

T. M. Hong
UCSB

S. Chen, J. Zhang
University of Colorado

D. Warner
Colorado State University

P. Trapani
Torino

M. Lu, N. Sinev, J. Strube
University of Oregon

S. Morganti, G Piredda, C. Voena
Roma "La Sapienza" University and INFN

H.P. Paar

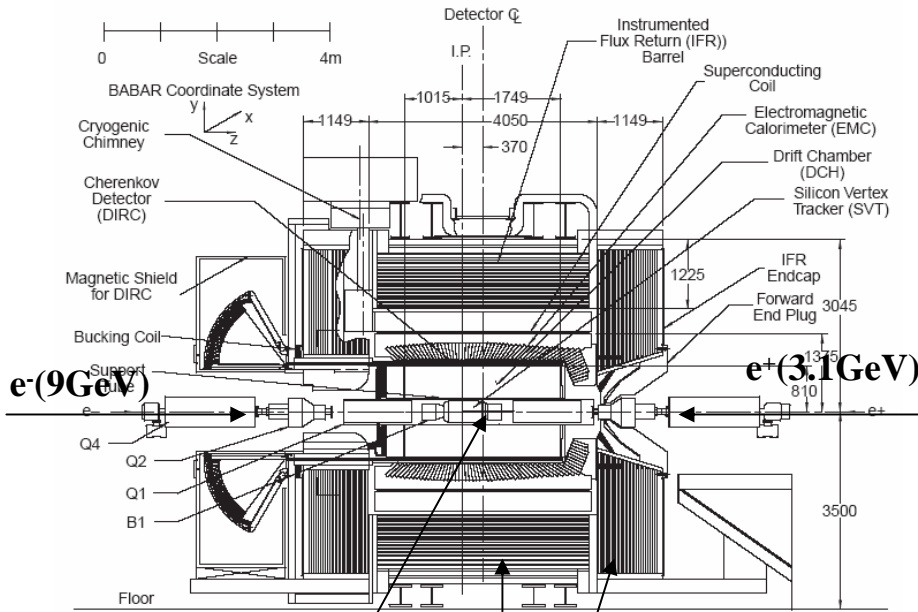
University of California at San Diego

R. Boyce, M. Convery, P. Kim, J. Krebs, R. Messner, M. Olson, R. Schindler,

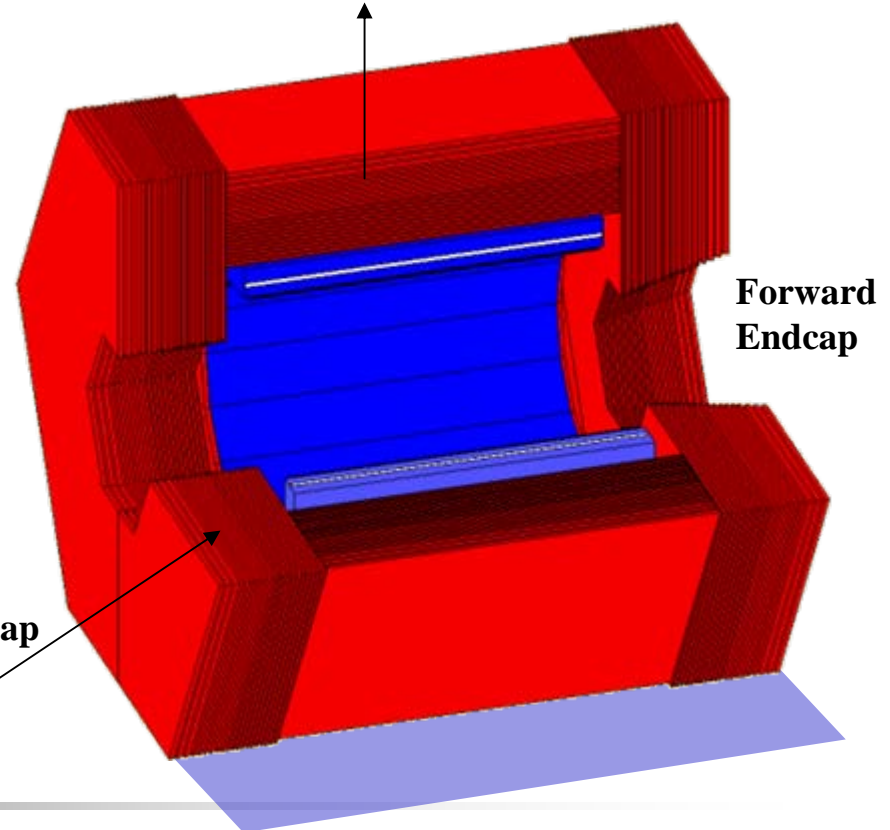
S. Swain, T. Weber, W. Wisniewski, C. Young
Stanford Linear Accelerator Center

IFR schematic

IFR → Instrumented Flux Return is the outermost and largest sub-detector in BABAR



Central Barrel Region
65cm of iron



Interaction Point

IFR

Backward Endcap
60cm of iron

Important Physics study using IFR detector (I)

Process	Physics Goals	Role of muons	Role of K_L^0	Comments
$B \rightarrow \pi \ell^- \bar{\nu}, B \rightarrow \eta \ell^- \bar{\nu}, \dots$	BR, V_{ub} , dN/dq^2	***		stat, high p
$B \rightarrow \rho \ell^- \bar{\nu}, B \rightarrow \omega \ell^- \bar{\nu}, \dots$	BR, V_{ub} , dN/dq^2	***		stat, high p
$B \rightarrow X_u \ell^- \bar{\nu}$ (with B_{reco} sample)	BR, V_{ub}	***		stat, high p
$B \rightarrow X_u \ell^- \bar{\nu}$ (incl. endpoint)	BR, V_{ub}	***		high p
$B \rightarrow \mu \nu, B \rightarrow \mu \nu \gamma$	BR, new phys	****	** (?)	stat
$D_s \rightarrow \mu \nu$	BR, f_{D_s}	****		high p
$\tau \rightarrow \mu \gamma$	New phys.	****		stat
J/ψ prod. w/init. state. rad.	leptonic widths	**		
$e^+ e^- \rightarrow \mu \tau$	New phys.	****		stat
$B \rightarrow K \ell^+ \ell^-$	BR, loops/new phys	****		stat
$B \rightarrow K^* \ell^+ \ell^-$	BR, loops/new phys	****		stat
$B \rightarrow X_s \ell^+ \ell^-$	BR, loops/new phys	***		stat
$B \rightarrow X_s \gamma$ (lepton tags)	BR, loops/new phys	**		stat
$B \rightarrow K \nu \bar{\nu}$	BR, loops/new phys		* (?)	stat

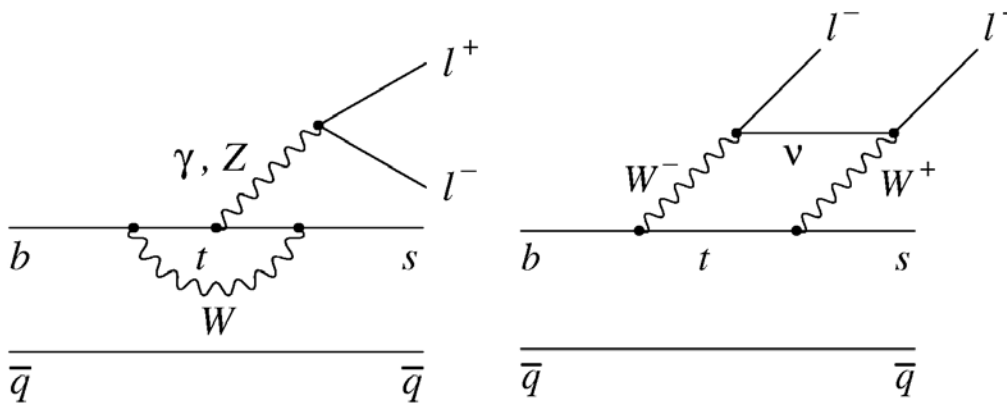
Rating system: IFR gives *(some benefit), ** (significant benefit),
 *** (large benefit), **** (essential information)

Modes highlighted in red will be discussed in more detail.

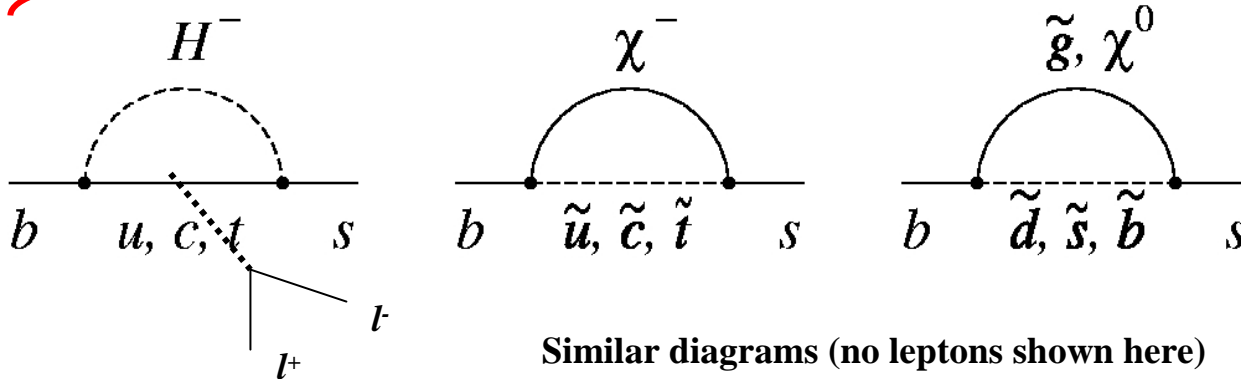
Important Physics study using IFR detector (II)

$B \rightarrow K \ell^+ \ell^-$, $B \rightarrow K^* \ell^+ \ell^-$, and $B \rightarrow X_s \ell^+ \ell^-$

Three diagrams in the Standard Model: penguins (g, Z), and the W^+W^- box:

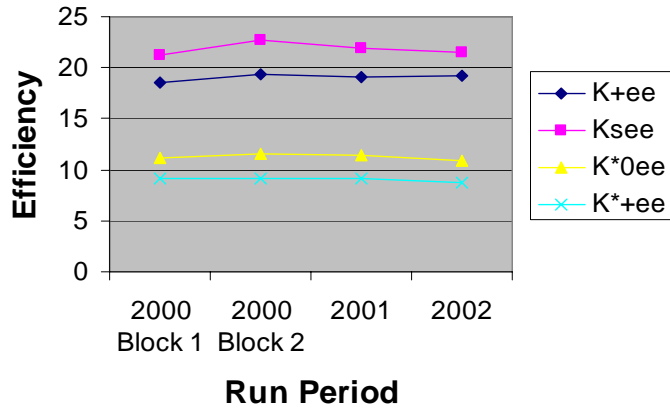


Possible new physics contributions



History of Electron & Muon Efficiency

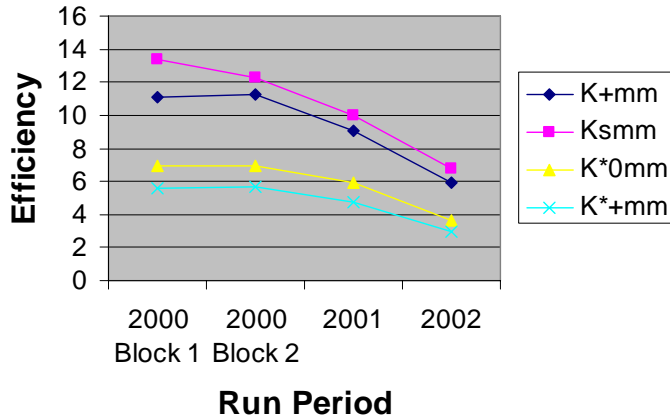
Analysis efficiency:
electron modes



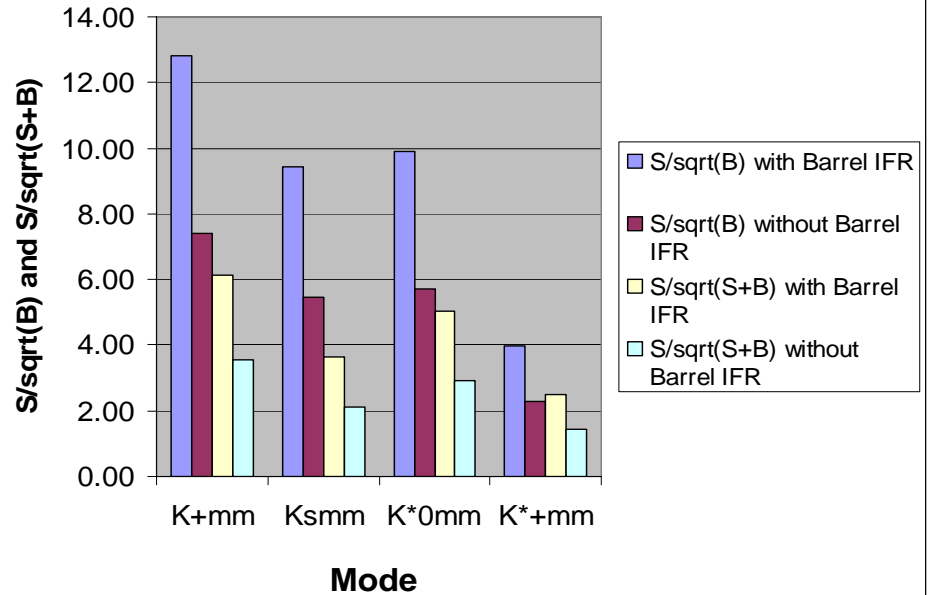
$K^{(*)}ee$ modes: ϵ stable

$K^{(*)}mm$ modes: ϵ lower and falling with time

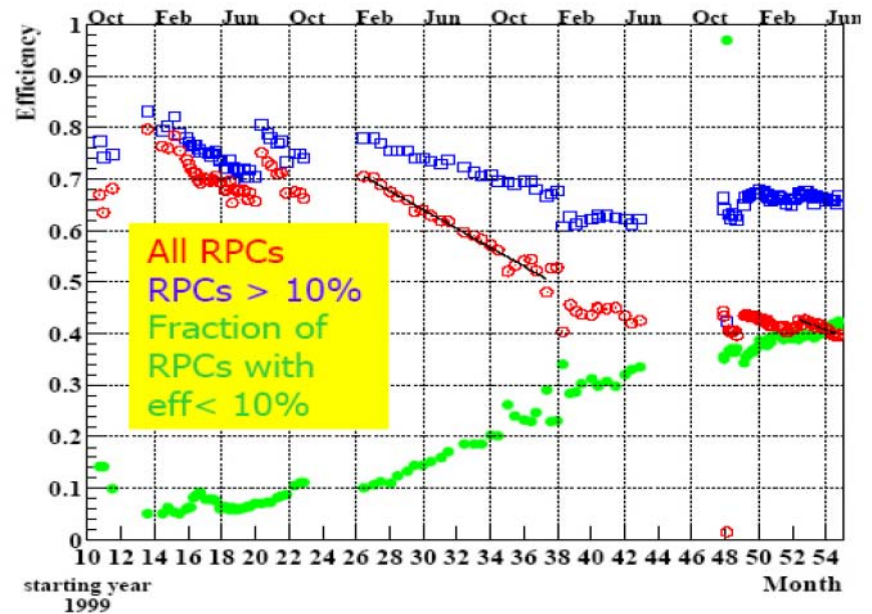
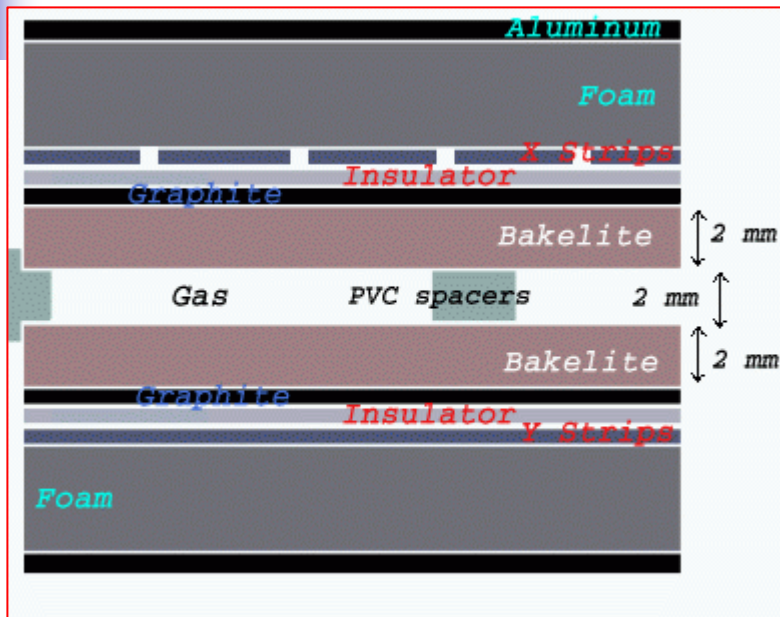
Analysis efficiency:
muon modes



Significance in muon modes with and without
Barrel IFR (500 fb⁻¹)



RPC flaws in BABAR



Large temperature increase in BaBar over short time.

Increase of dark current/noise, reached current limits.

RPC efficiency drop (right plot)

The readout electronics inside the detector volume

(For details please see [Chang-guo Lu's talk](#))

Upgrade of IFR detector

I will discuss
the barrel upgrade

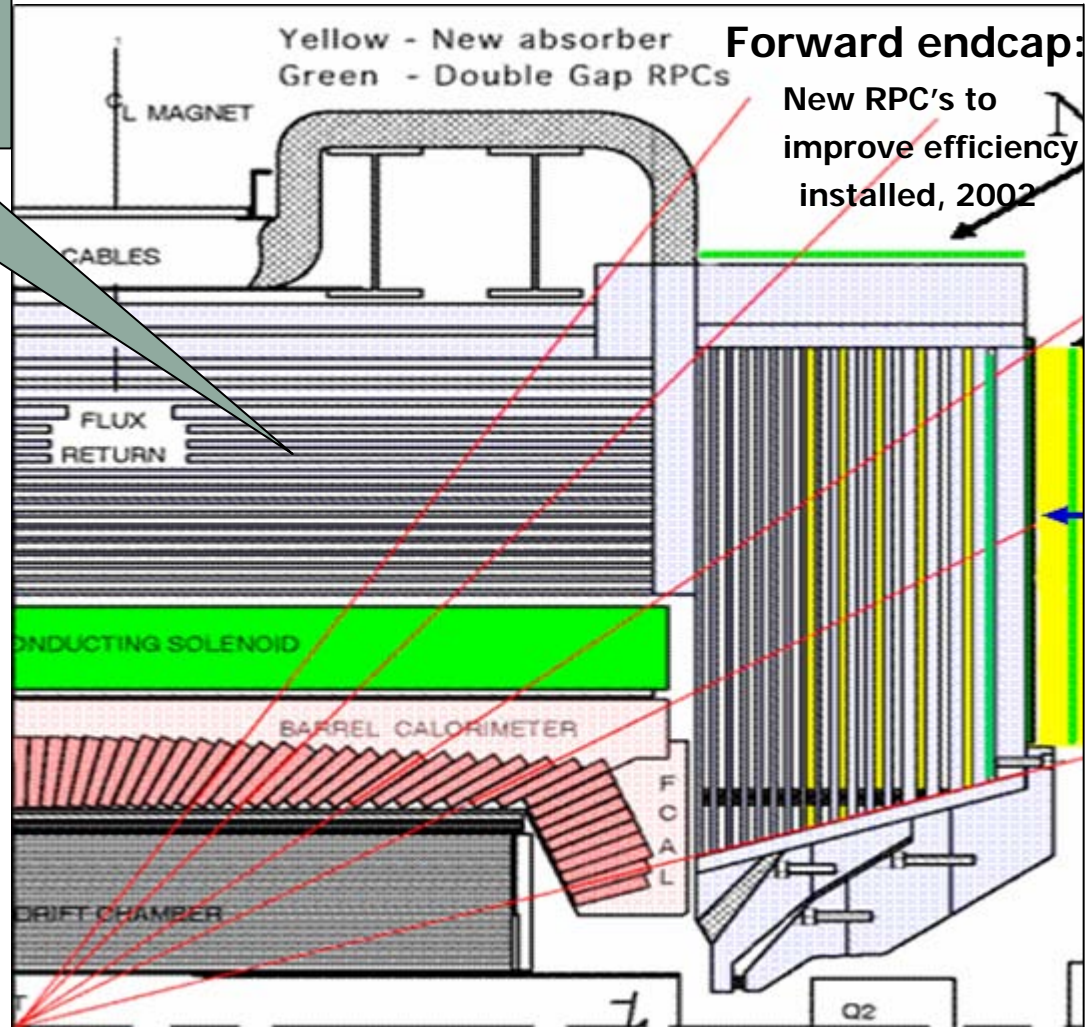
12 layer RPC → LST

6 layer RPC → Brass

Layer 19 not accessible

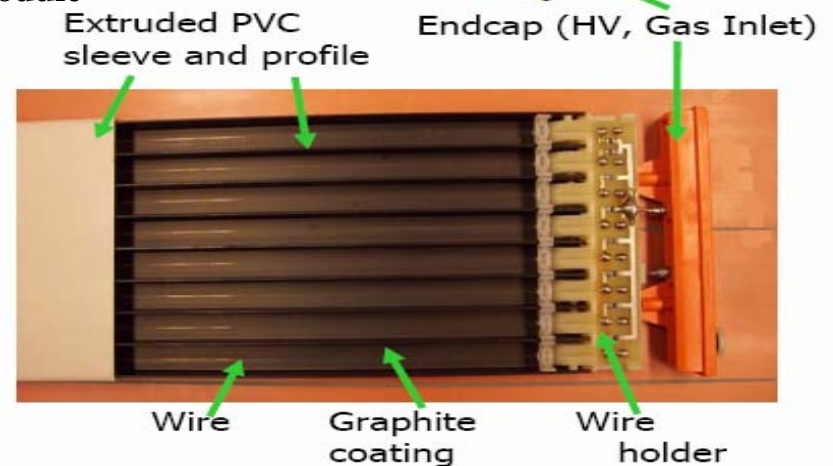
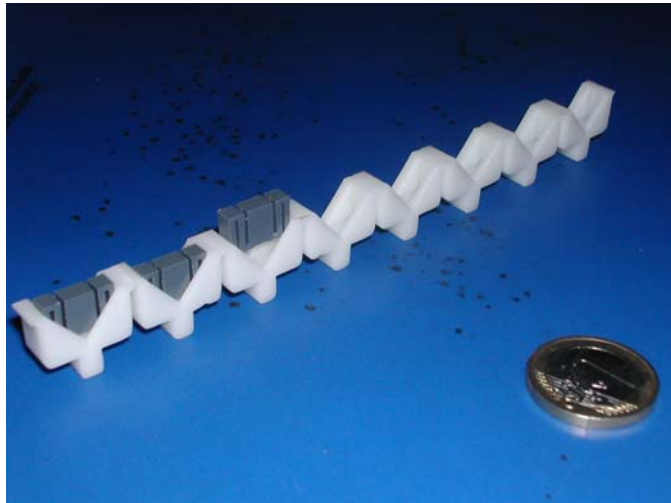
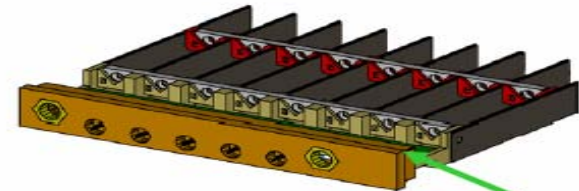
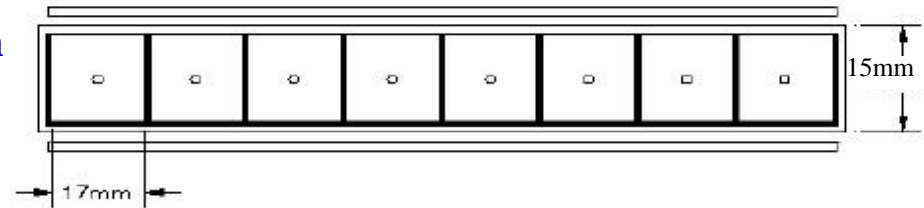
2 sextants in 2004

4 sextants → 2006



Limited Streamer Tubes (read out ϕ coordinate)

- Tubes consist of 7 or 8 cells
- Cell dimensions: 15mm x 17mm x 3.6m
- Consists of gold-plated anode wire and graphite-painted PVC walls (cathode)
- Enclosed in PVC sleeve
- Endcaps include HV / gas connections
- Produced at pol.hi.tech company in Italy.
- At Princeton and OSU, the tubes are glued onto a SLAC-produced “phi-plane” to form module

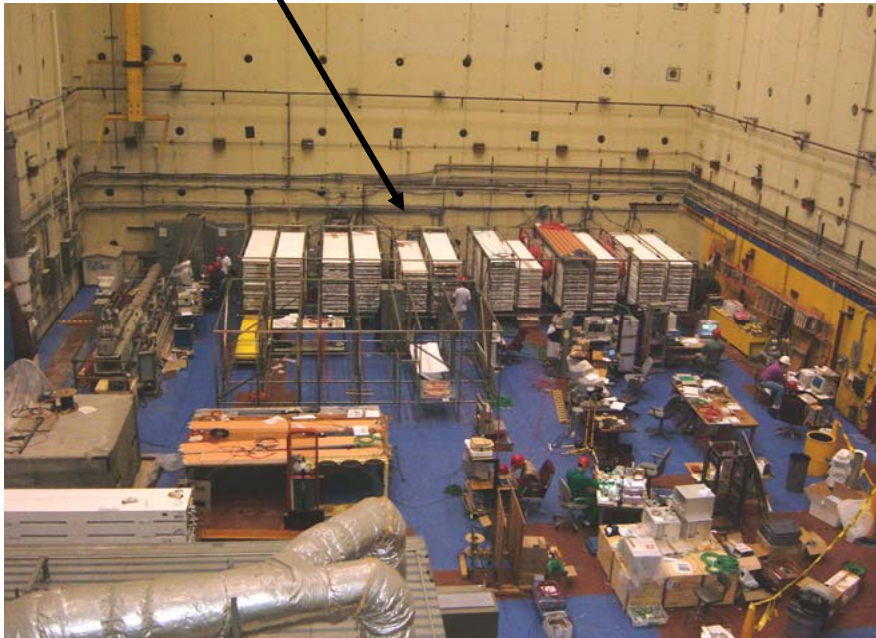


LST Module and Q/C test

A Layer within a sector consists of 6 to 10 LST modules
Each module contains of 2 or 3 8(7)-cell Tubes

The 3 different types of modules arranged
to minimize the dead space

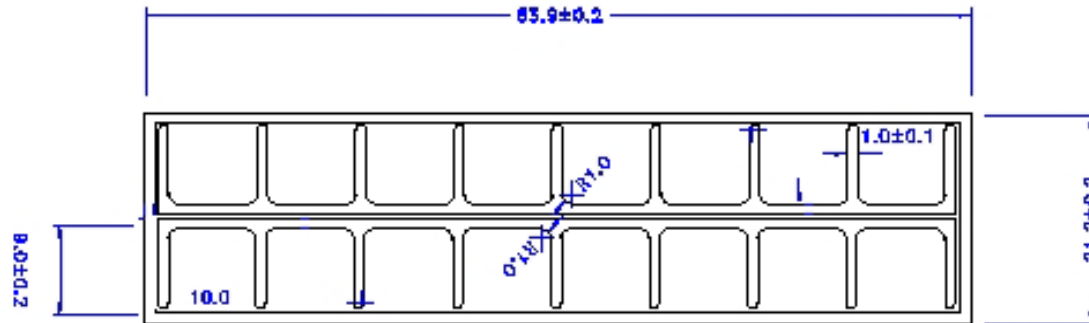
We Q/C the modules before putting into the detector



Options for module design

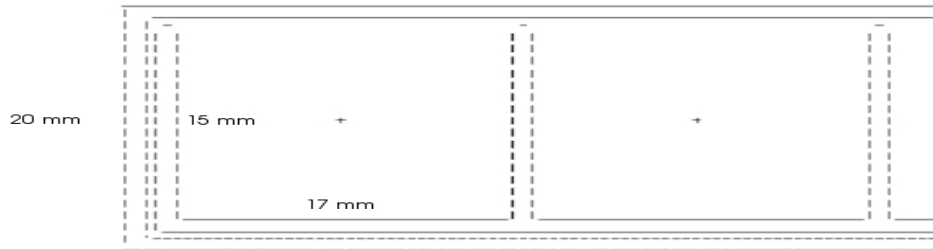
Option 1: Double-layer with a small cell (9mm x 8mm)

Reading out both coordinates from outside strips is possible



Option 2: Single-layer with a large cell (17mm x 15mm)

Readout one coordinates from outside strips (BABAR case)



Single layer has low mechanically failure rate, simpler HV and Gas system , and cheaper than double layer .

There will be some efficiency loss from double -> single layer LST.

Making the cell size bigger compensates this loss (9mm x 8mm -> 17mm x 15mm).

Effect of wire diameter to the e-field on wire surface

Anode wire diameter variation has big impact to the e-field on the wire surface.

The e-field on the wire surface:

$$E(R_a) = \frac{V}{R_a \ln(R_c/R_a)}$$

$$\Delta V = V \frac{dE(R_a)/dR_a}{E(R_a)} dR_a = -V \frac{\ln(R_c/R_a) - 1}{R_a \ln(R_c/R_a)} dR_a = \left[-V \frac{\ln(R_c/R_a) - 1}{\ln(R_c/R_a)} \right] \frac{dR_a}{R_a}$$

Assume $V=5000V$, $R_c=0.6cm$,

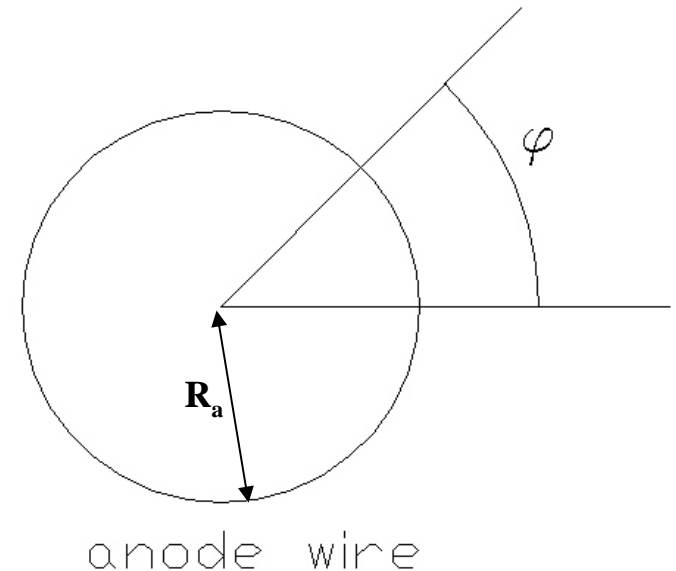
If $dR_a/R_a = 5\% \Rightarrow \Delta V = \sim 200V$

5% of wire diameter increase leads to 200V effective voltage drop on the wire.

This has impact on the plateau curve.

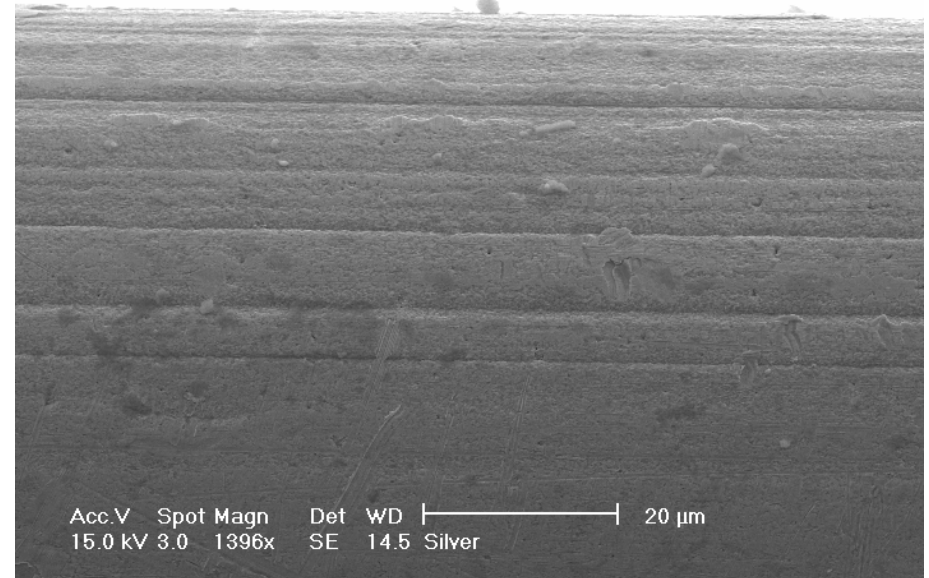
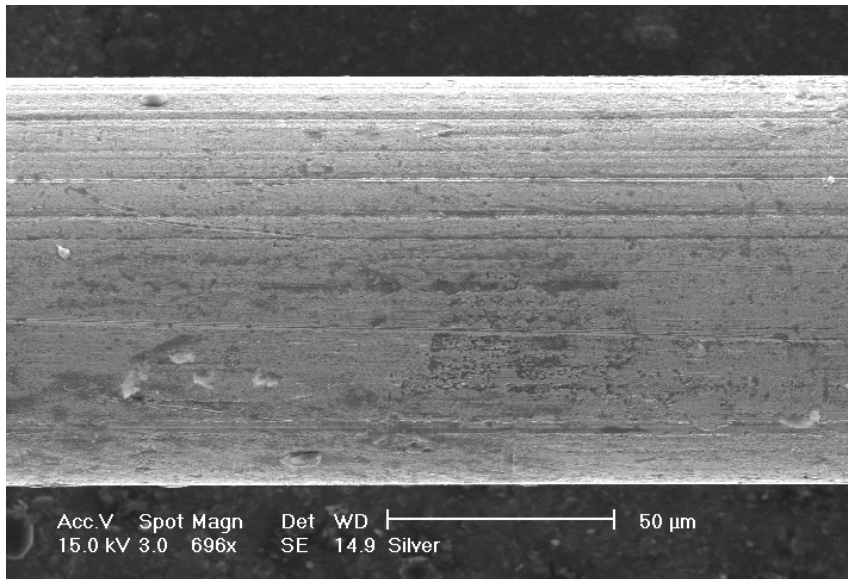
Apart from wire diameter, one has to look at smoothness of wire

Other important aspect is to look into aging effect for the wire.



Images of Au-plated Be-Cu wire

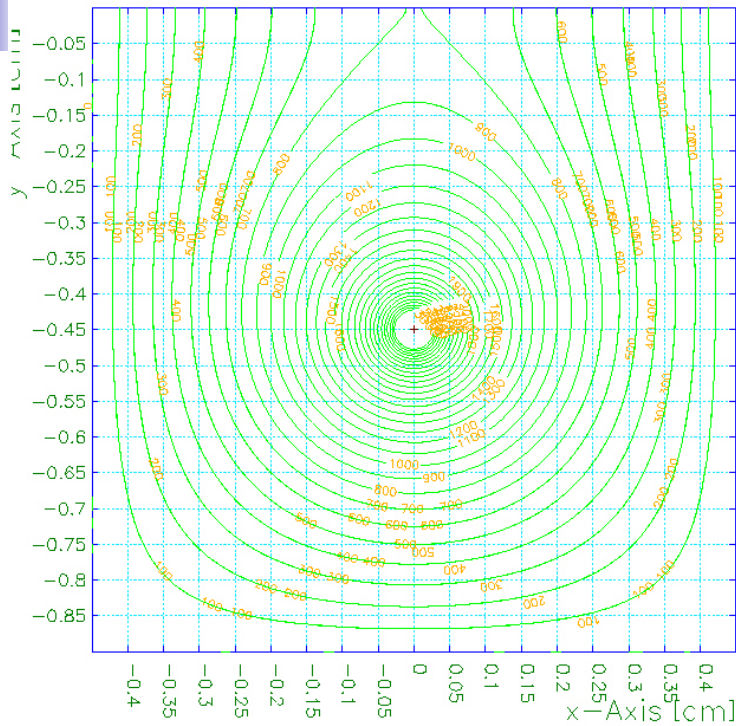
The following pictures using Phillips XL30 FEG-SEM electron microscope and PGT-IMIX PTS EDX x-ray analysis system at Princeton Image and Analysis Center .



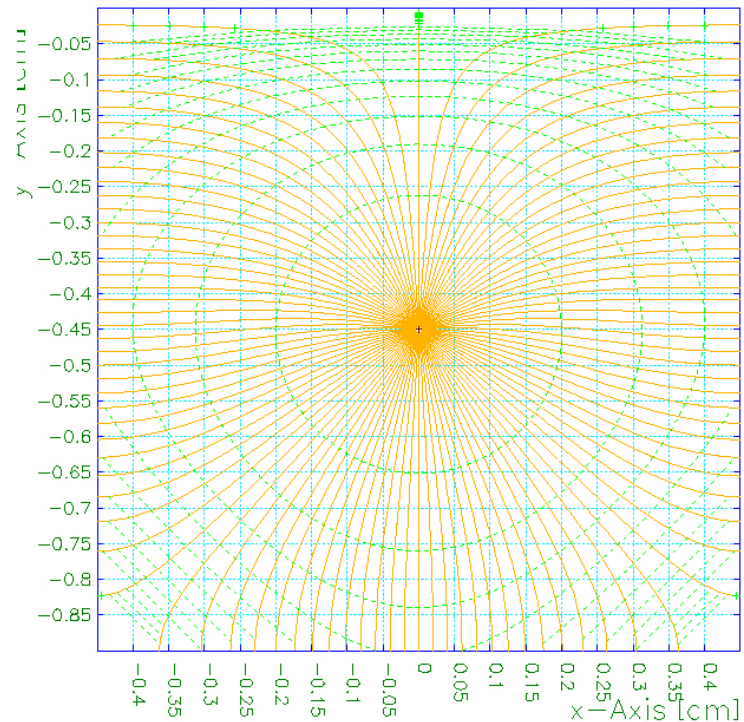
Use SEM scale measured wire diameter is 101μm, micrometer measured is 97 μm.

For Ag-coated wire, SEM scale measured diameter is 107μm and micrometer measured 105μm

LST grounding (coverless tube)



V contour plot



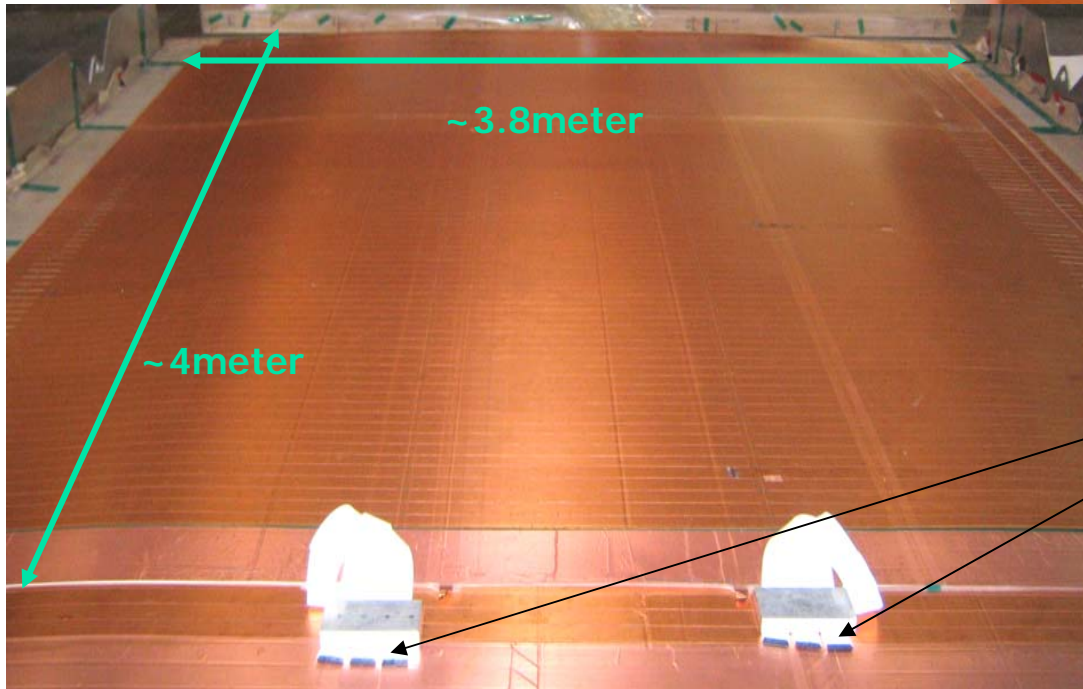
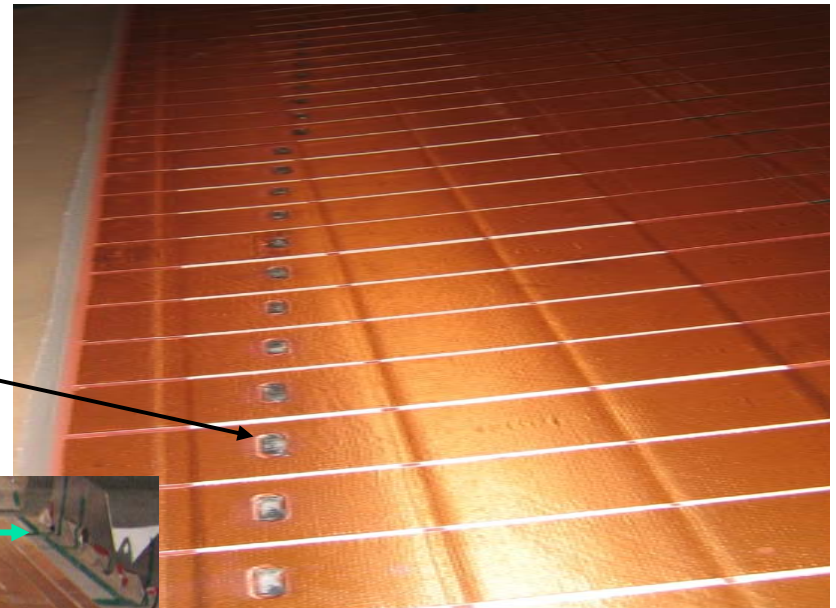
E-field lines

The top shielding is not only for the read out of LST, but also is an essential part of LST tube. With and w/o this shielding an LST can behavior quite differently. In our case, LST is attached to ϕ -plane so that it is always grounded on the top.

Z-coordinate readout planes

1mm thick vacuum laminated planes made with Cu foil + Mylar

35mm wide 96-strips connected to cables (2mm gap between strips)



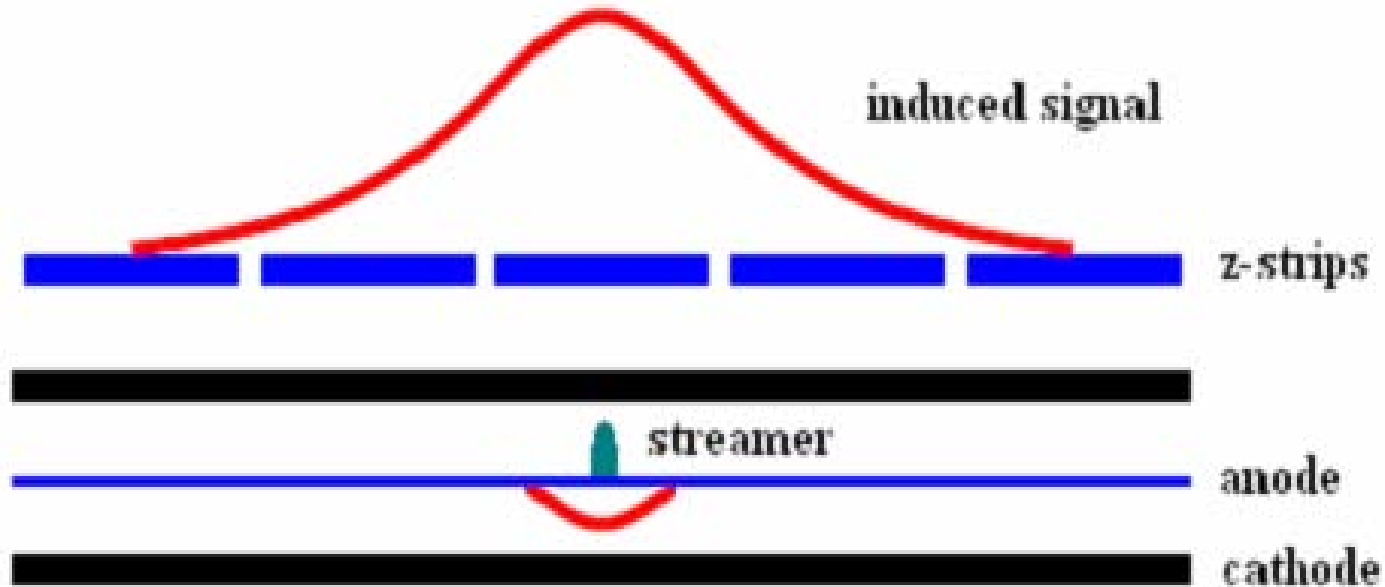
16 channel cables for signal pick up
(6 cables: 3 on Each side=96strips)

These planes are built at SLAC

23rd August-2005

ALCPG, Snowmass, Colorado

How does LST work ?



Segmented strips adjacent to detector pick up induced charge signal from the streamer

Anode wire signal can be read out directly from on top of HV

This yields two position coordinates. The third is gained by installing multiple layers of streamer detectors. Combined, these allow full tracking

LST installation

Simple Procedure:

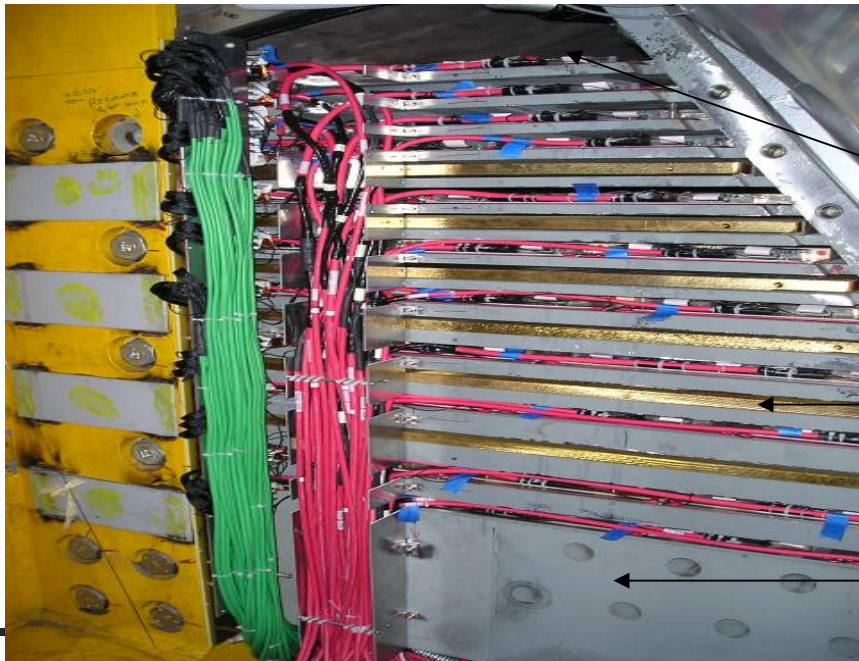
1. Insert Z-planes
2. Push the Modules inside the gap



**Test them before
completion of layer**

Backward view of bottom sextant

The empty iron gaps inside the IFR before installation (after RPCs are being removed)



All the layer after LSTs are installed

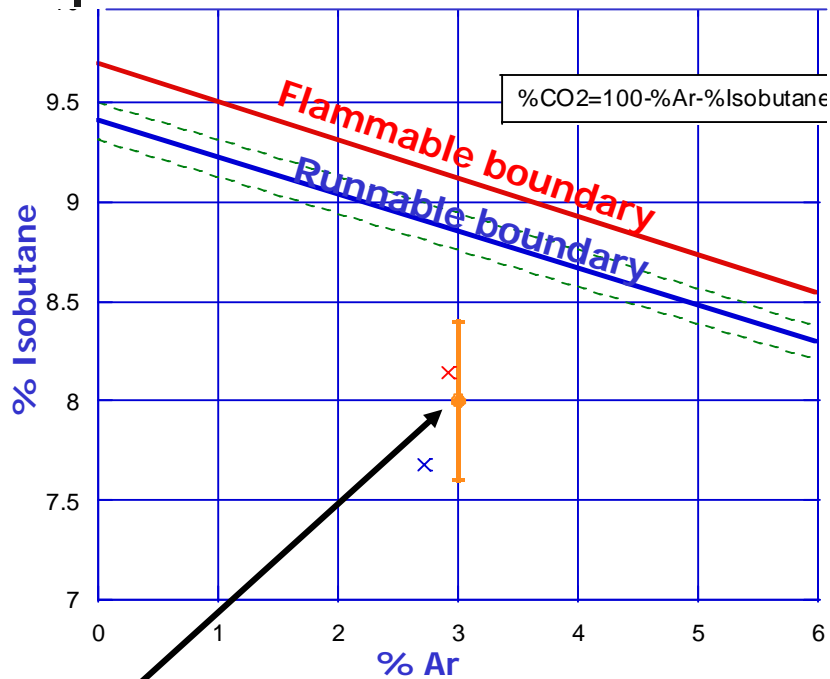
Brass slab

Layer-18 inside the iron block (not accessible from the backside)

23rd August-2005

ALCPG, Snowmass, Colorado

Gas System



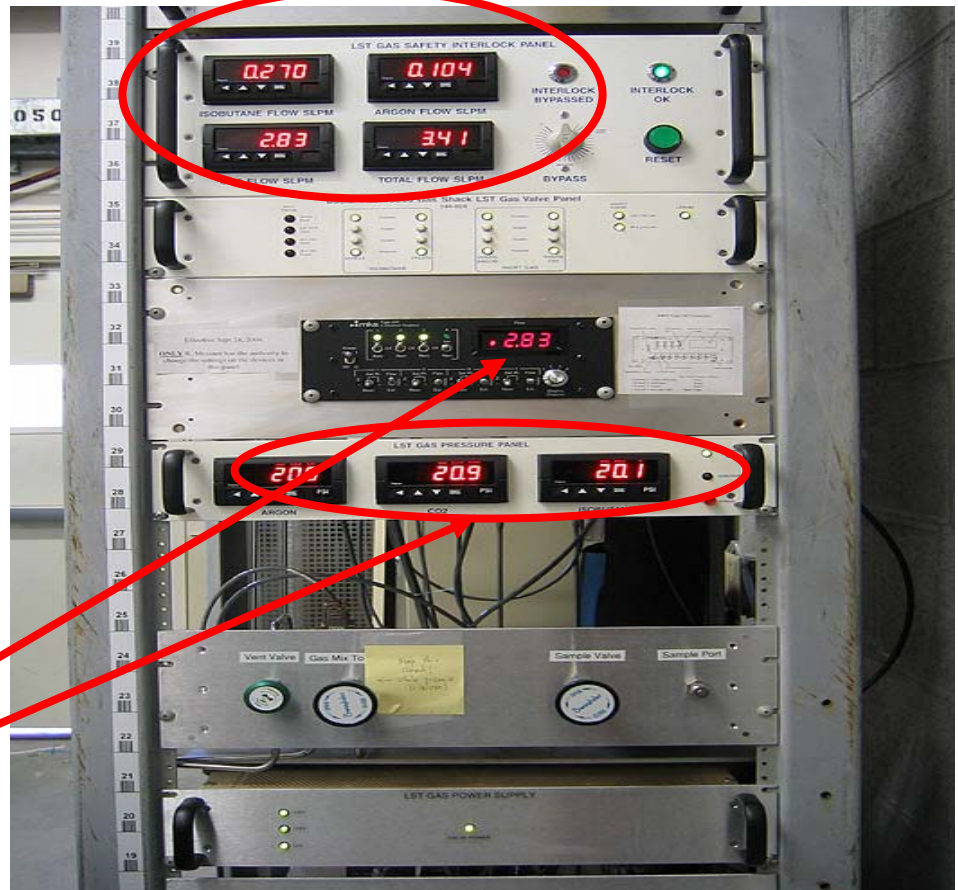
Gas: CO_2 -89% /Ar-3% /Iso-8%

Mass flow controller

Pressure monitor

Gas controller and monitor

Monitors mass flow meters



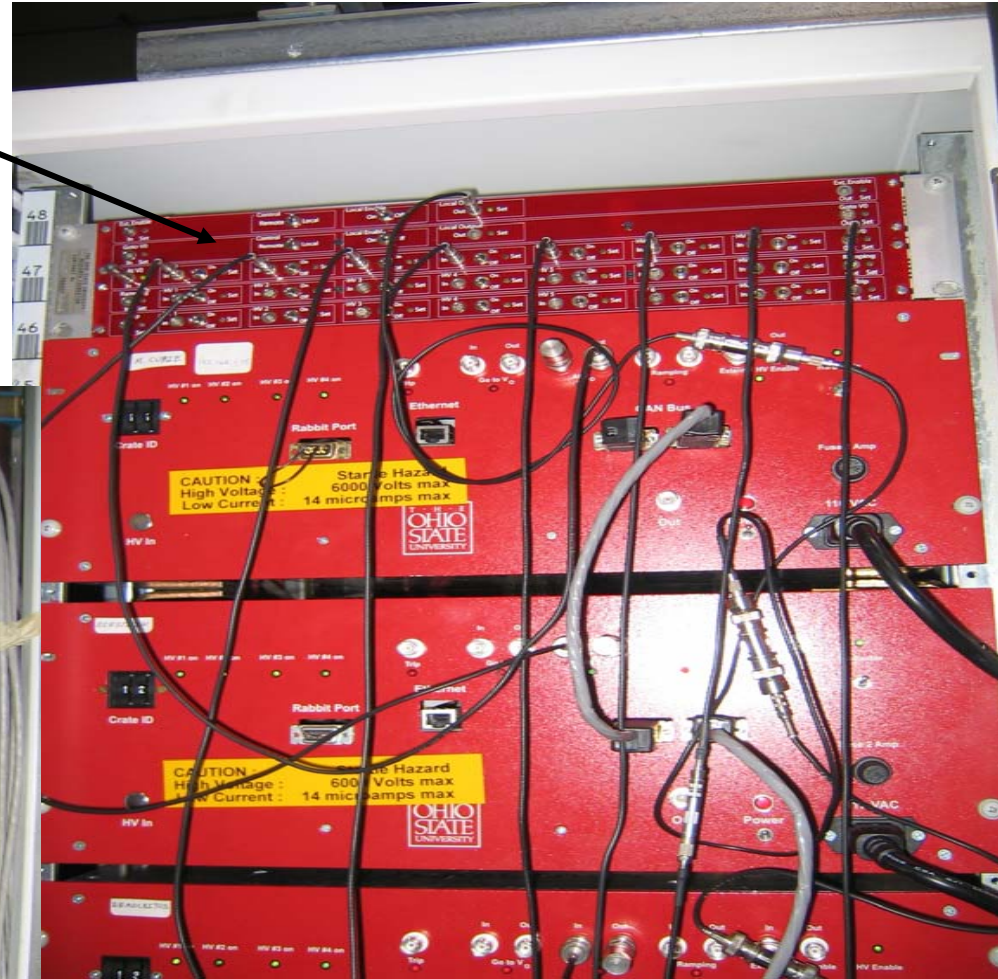
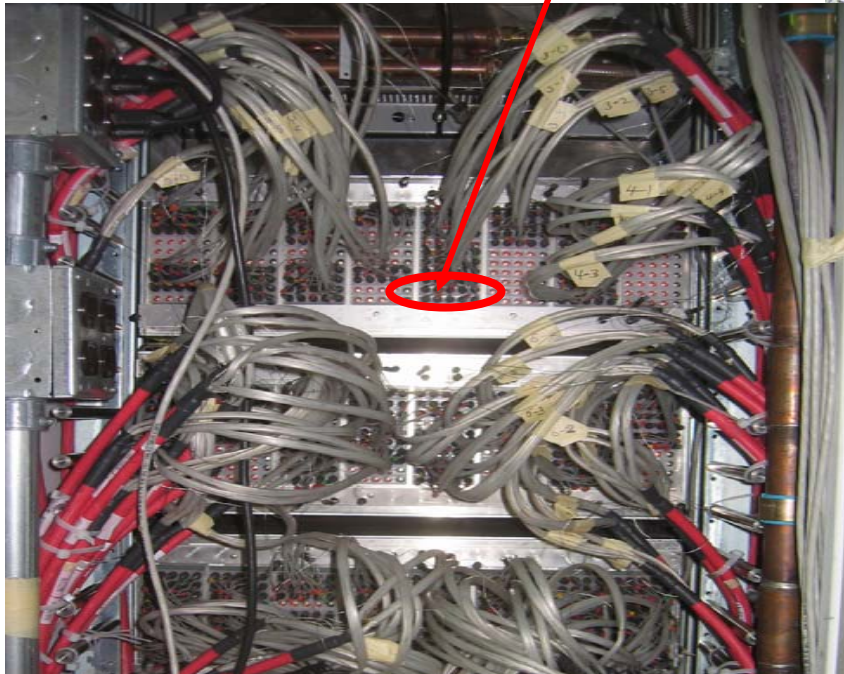
High Voltage

Enable and control box for HV

High Voltage system provides a 4 channels
for every tube

Costume made by OSU

→ granularity

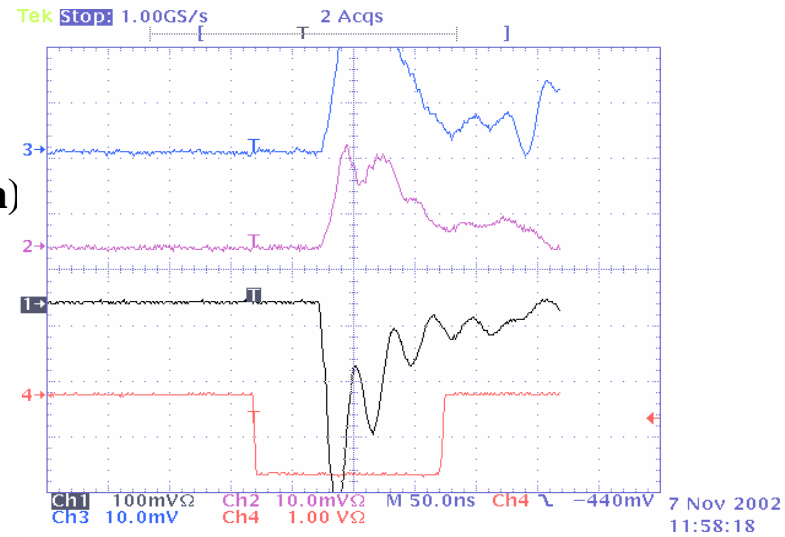
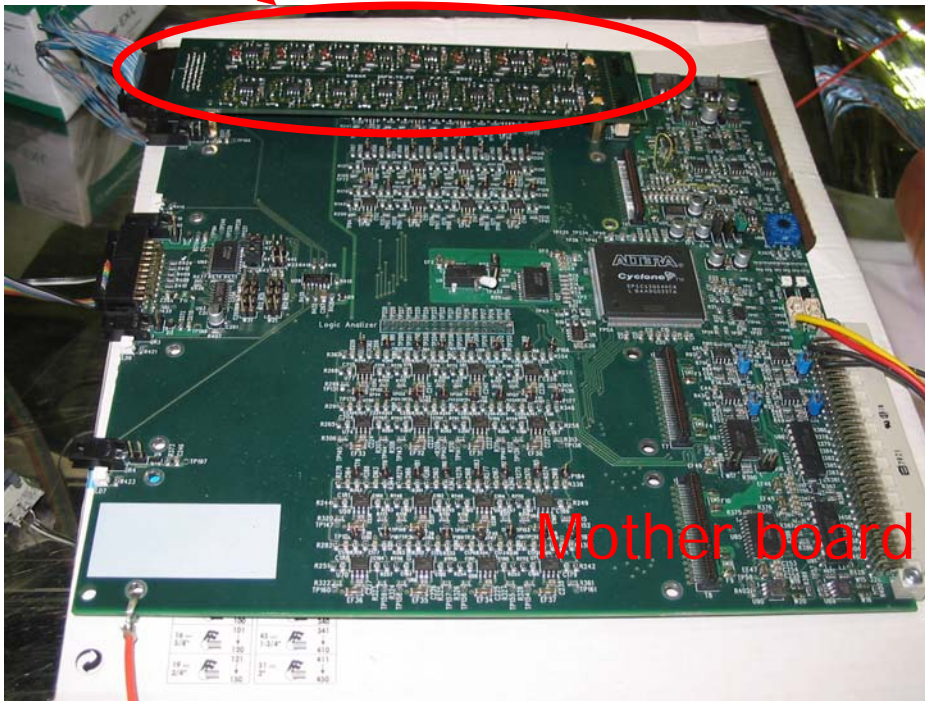


Readout boards

A completely new electronics has been developed to readout the signals from:

- strips (z coordinate – beam line direction)
positive signal
- wires (phi coordinate – azimuthal angle)
negative signal

Daughter board

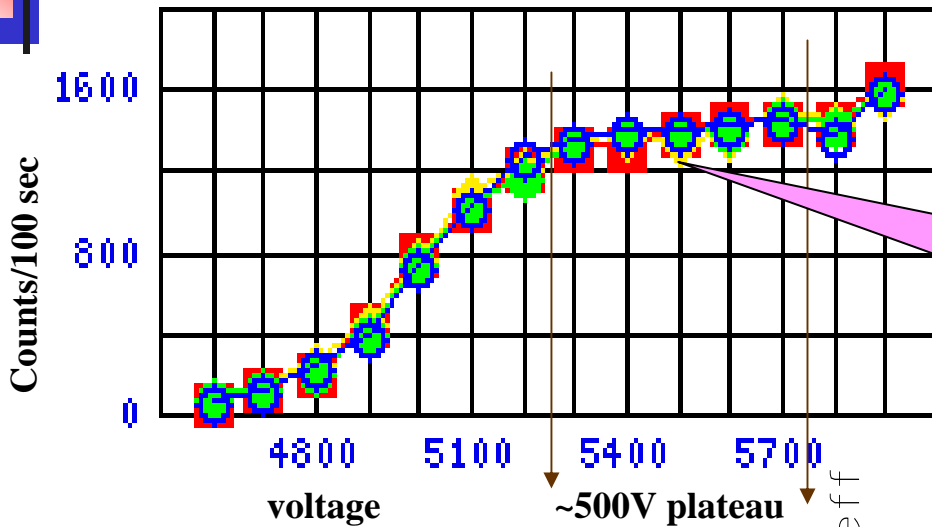


Signals are sent to Front End Cards
and there amplified and discriminated.

In case of RPC, the front end cards were inside
detector volume

→ Not accessible once detector is closed

Detector Performance (I)



All the 4 channels in every tube are consistent with each other

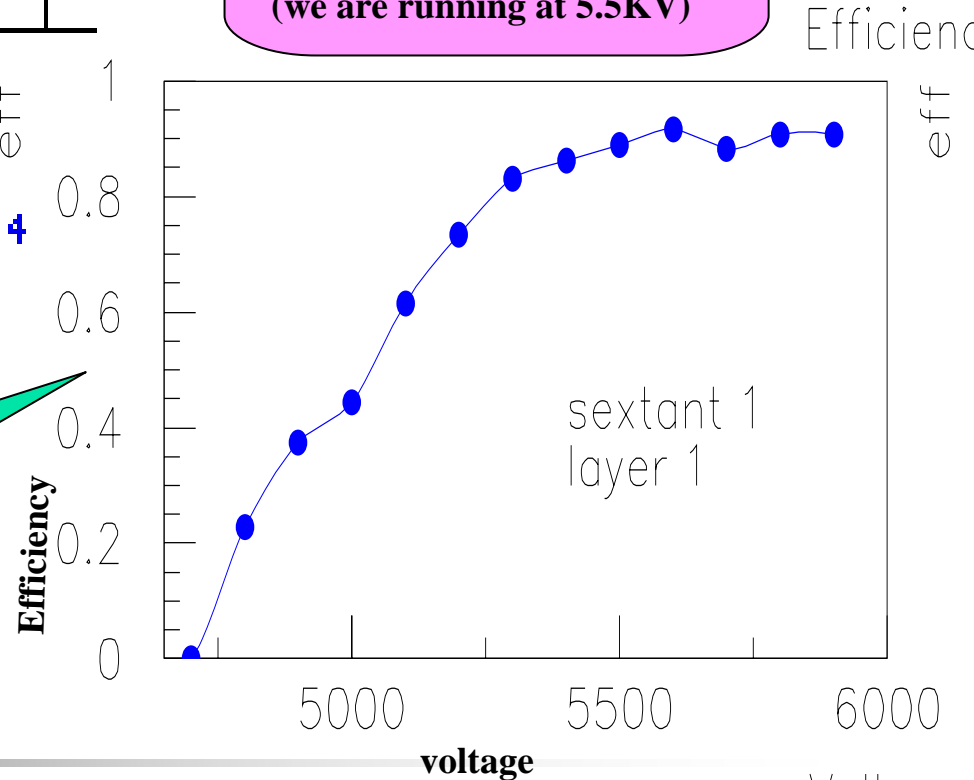
All the modules and tubes are working good.

Singles rate for a tube in Layer#18

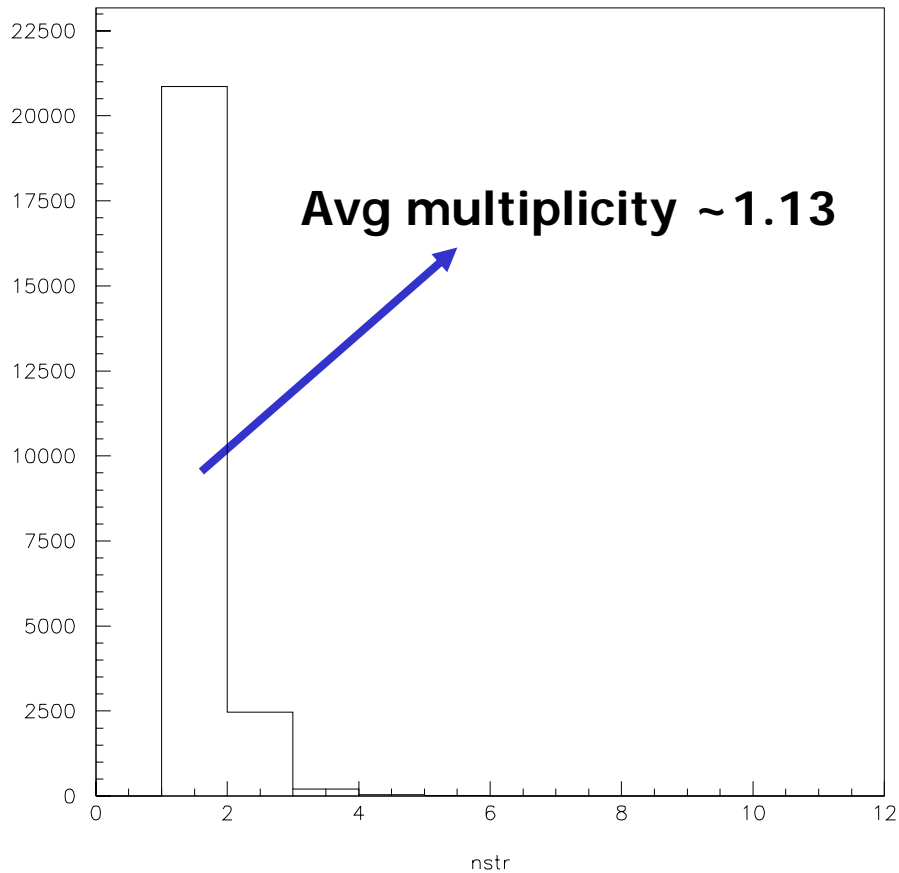
Nice plateau ~ 500V
(we are running at 5.5KV)

Ch 1 Ch 2 Ch 3 Ch 4

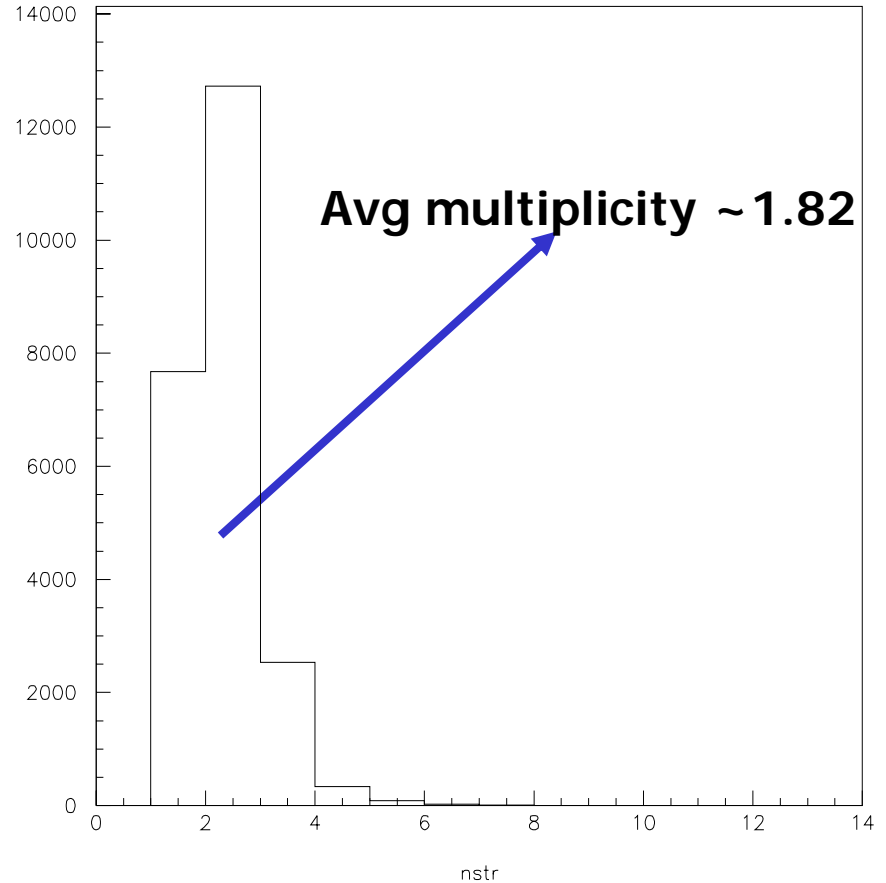
Average layer efficiency ~92%
(from cosmic data)
Consistent with LST geometry



Wire and Strip multiplicity



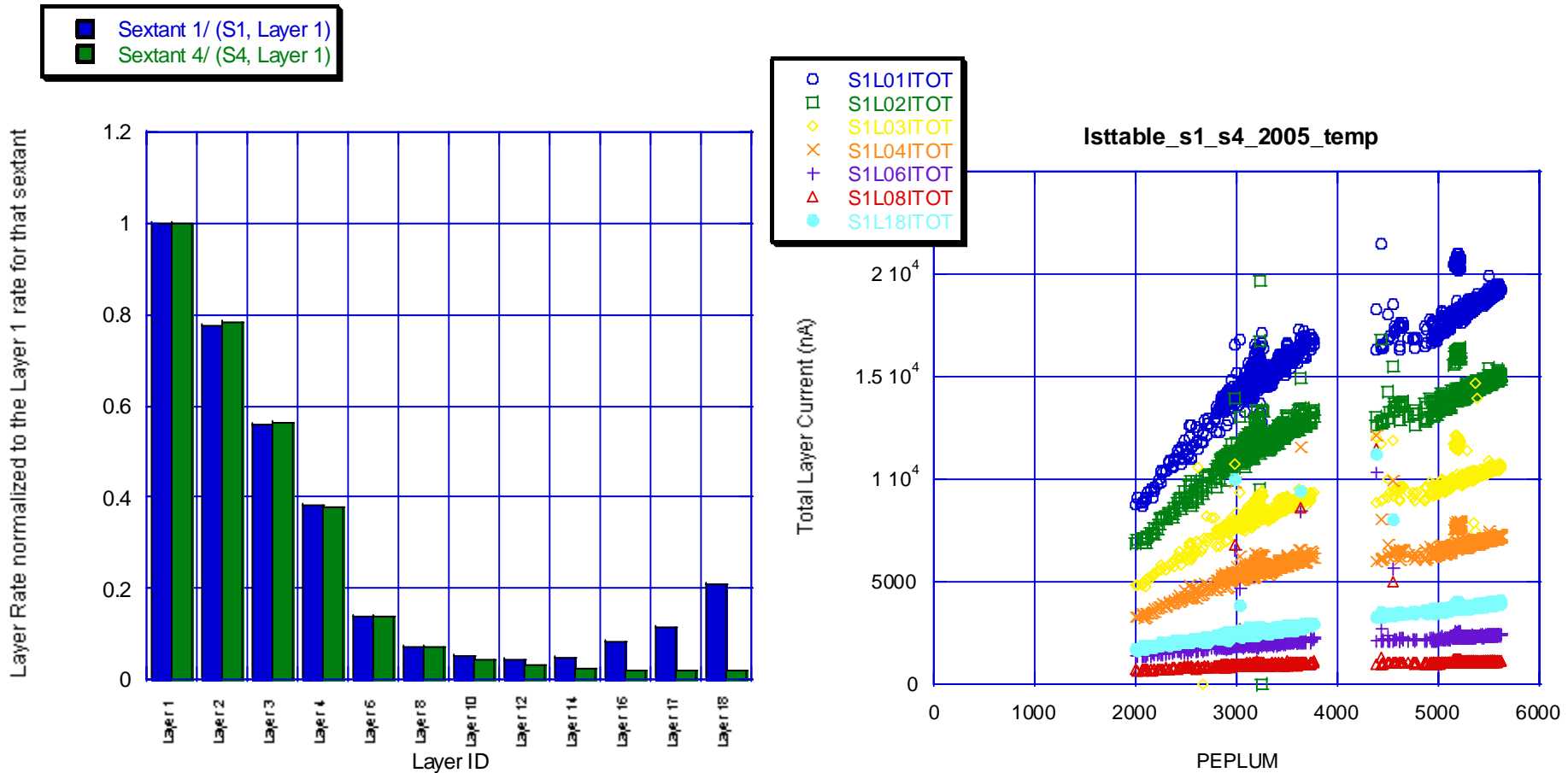
Wire Multiplicity



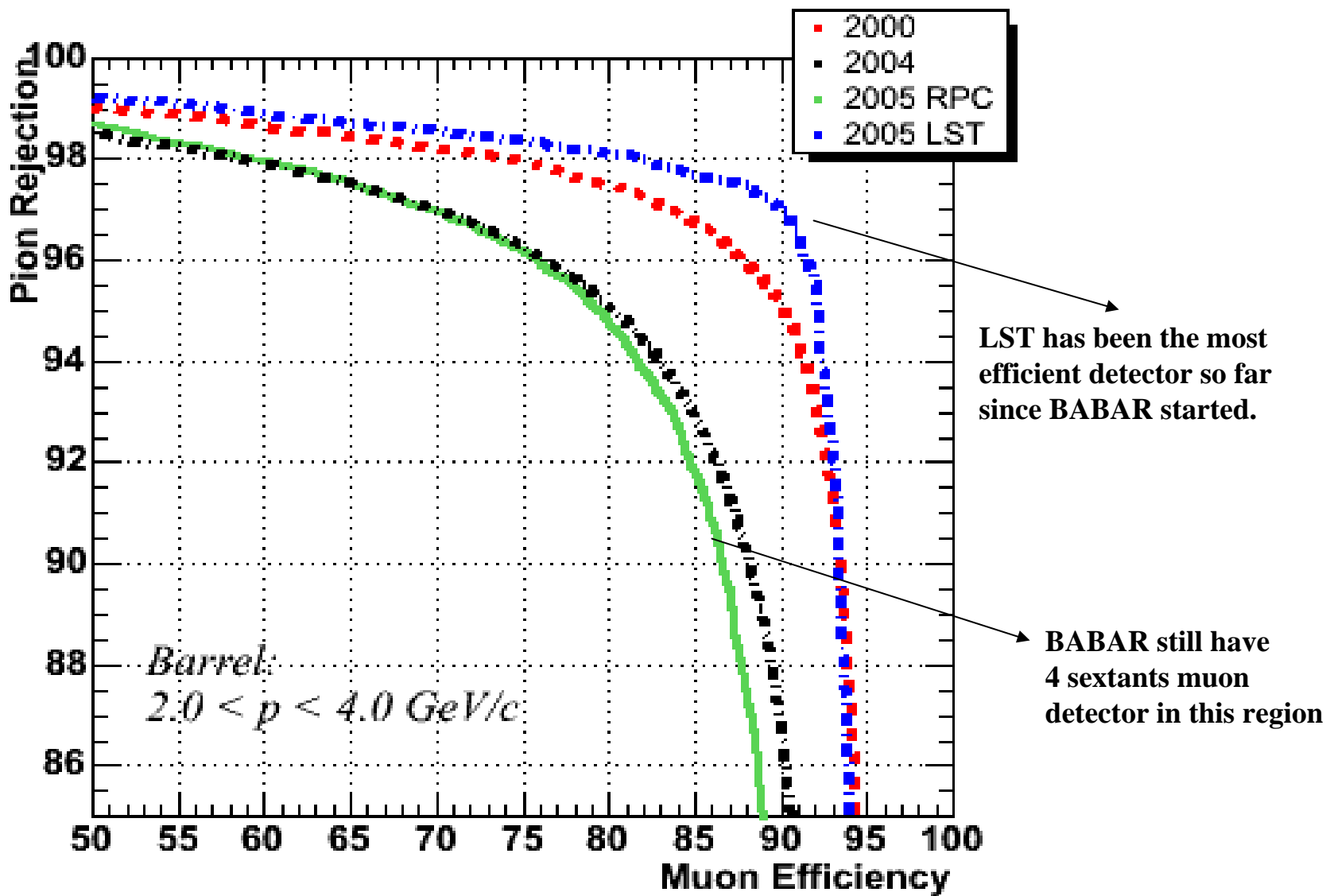
Strip Multiplicity

Counting rate and Currents versus luminosity

Plots are obtained from the BABAR run during Apr 18th-25th, 2005.

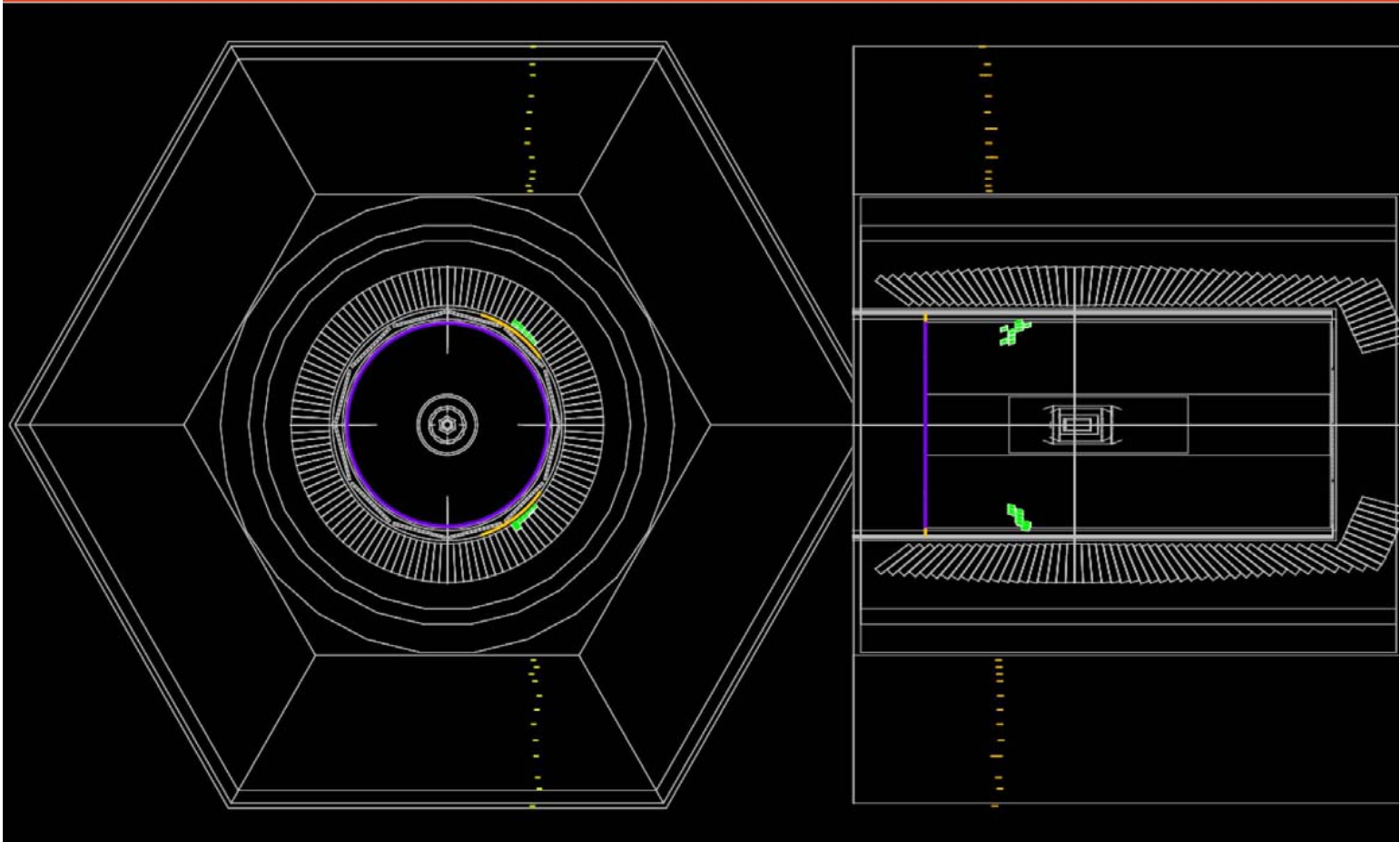


Improvement of muon efficiency



Cosmic Ray Muon in New BaBar IFR

Sept 30, 2004



Summary

We installed 2 sextants in 2004 (top and bottom)

→ 388 tubes: 1552 readout channels

→ **All, except 5, of them working good**

→ 24 Z-planes: 2284 strips

→ **0.7% disconnected channels (not adjacent strips)**

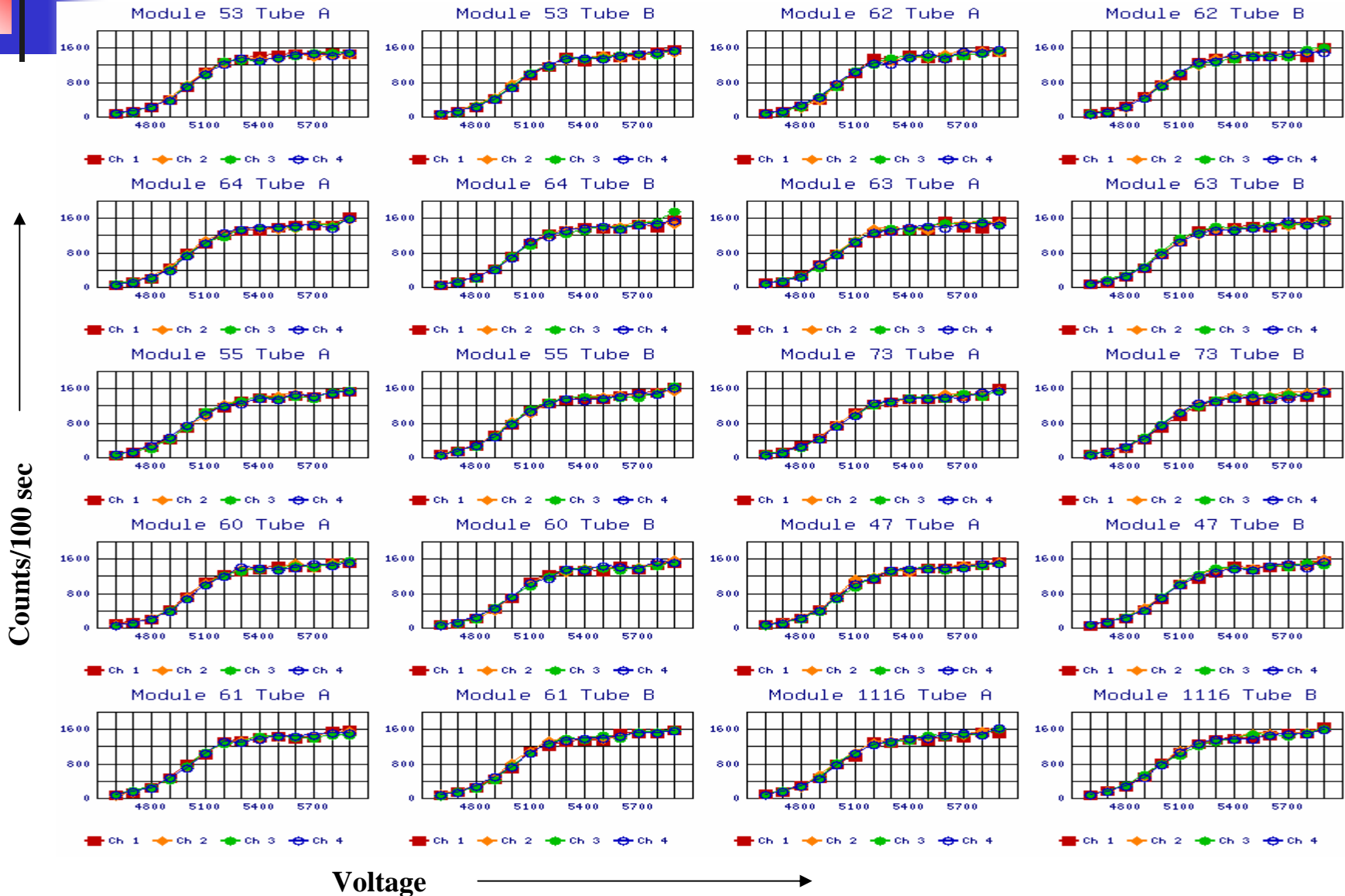
→ no efficiency loss (strip multiplicity is ~1.8)

2/3rd of the Barrel to be installed in 2006

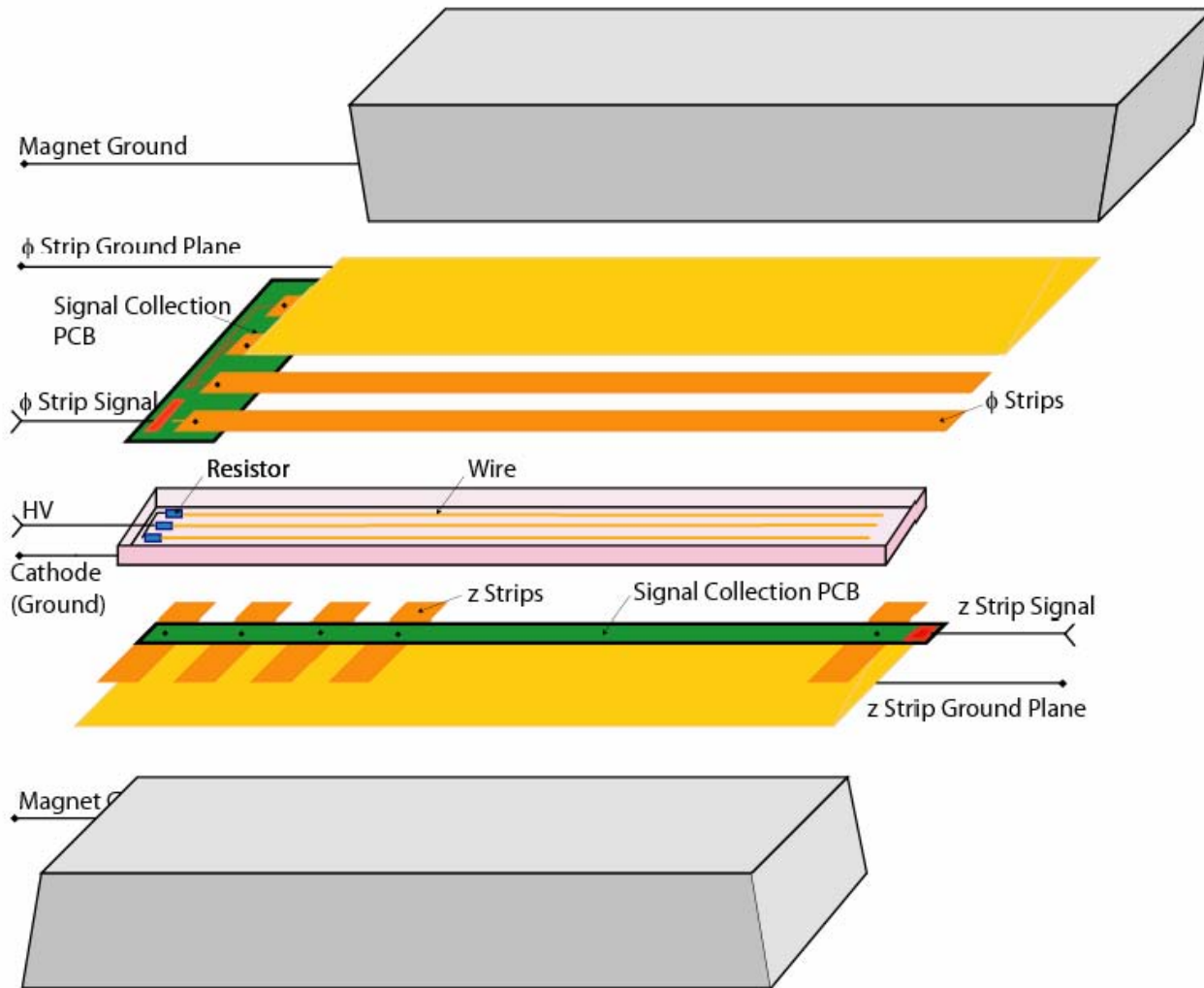
→ bigger challenge because it is tilted
(pushing the z-planes and modules
requires special instrumentation)

**But the experience during last year installation will be
advantageous for next year installation**

Plateau measurement for Layer#18 modules



Possible LST configuration inside the iron gap

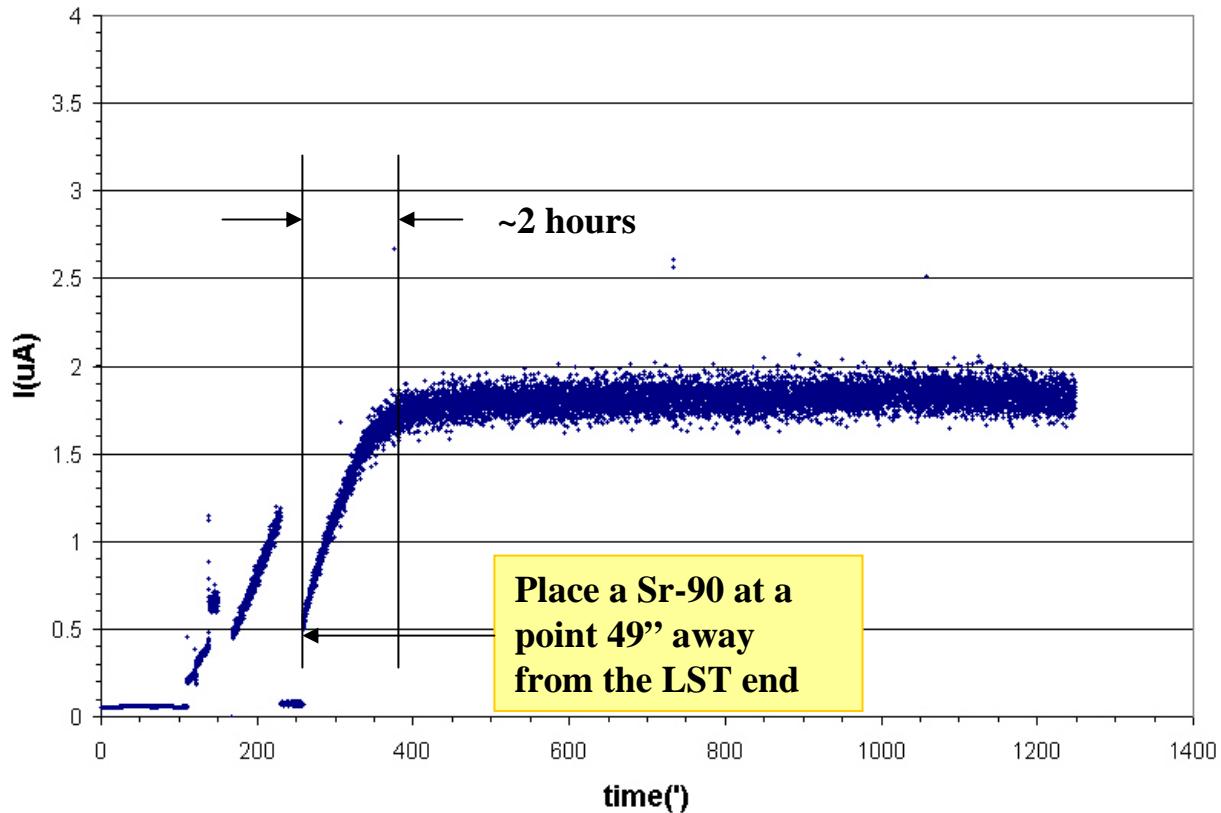


One can read out the z and f coordinate of the hit through the strips in both direction but for our case, the ϕ signal is read through the anode wire rather than ϕ -strips

Shielding of LST

W/o top shielding anode current increasing with time

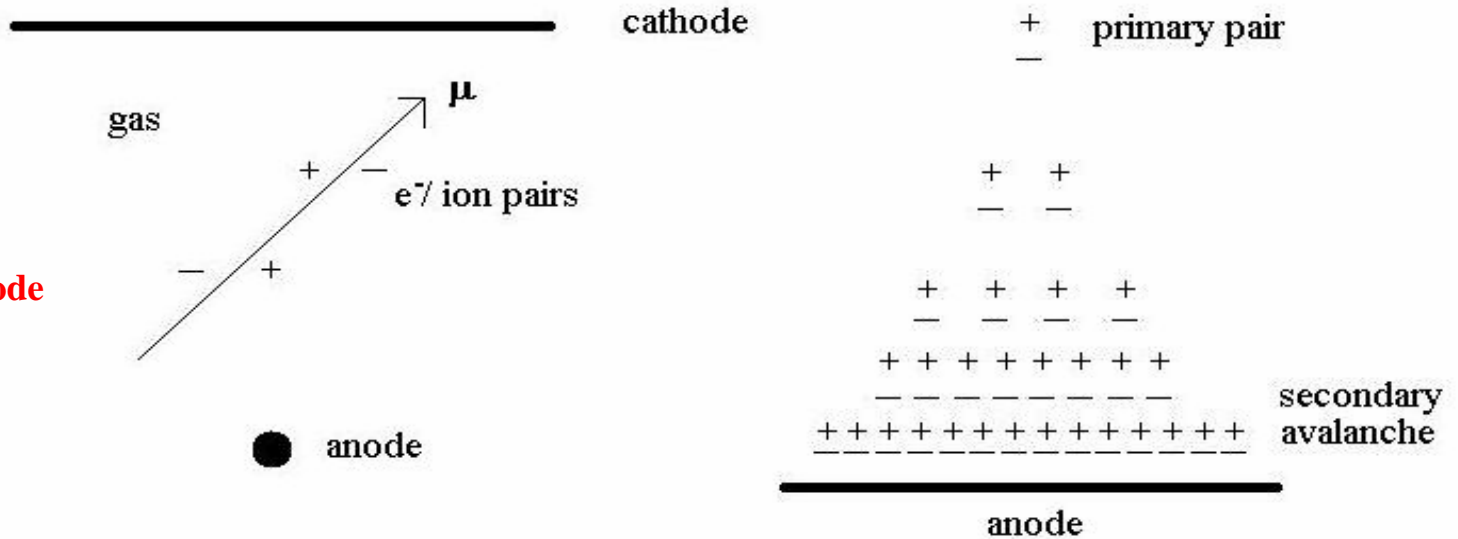
It takes ~ 2 hours to stabilize the current, the final current is much higher than the initial current:



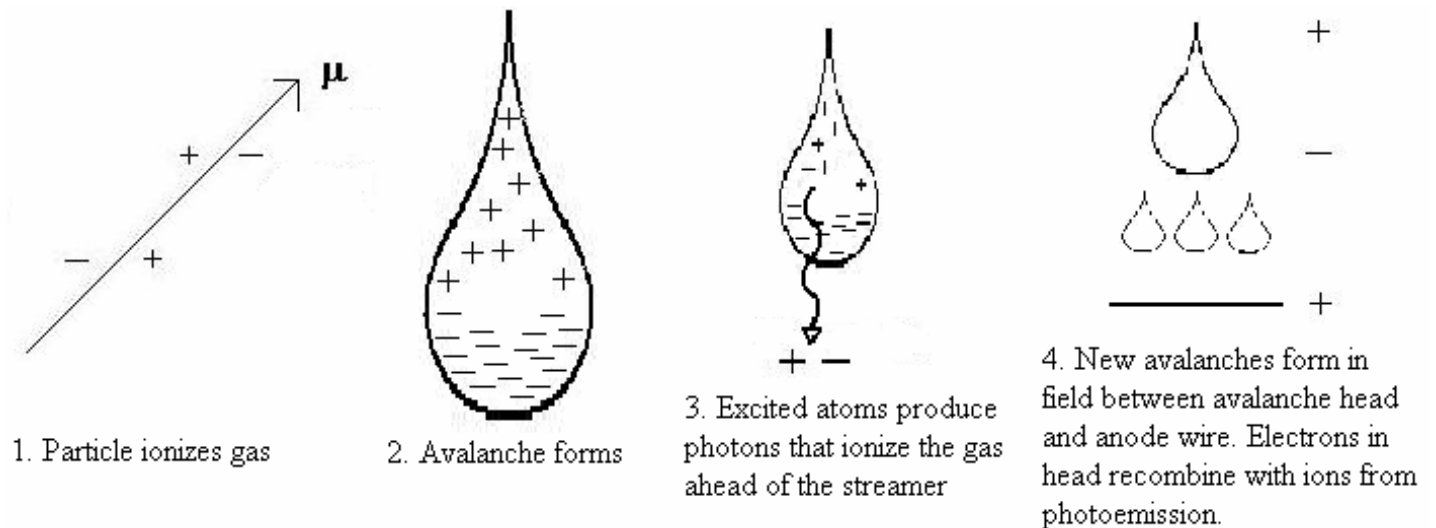
W/o grounded shielding on the top of LST, under intensive source radiation the anode wire current takes ~ 2 hours to get stabilized.

Why to run the detector at Streamer Mode ?

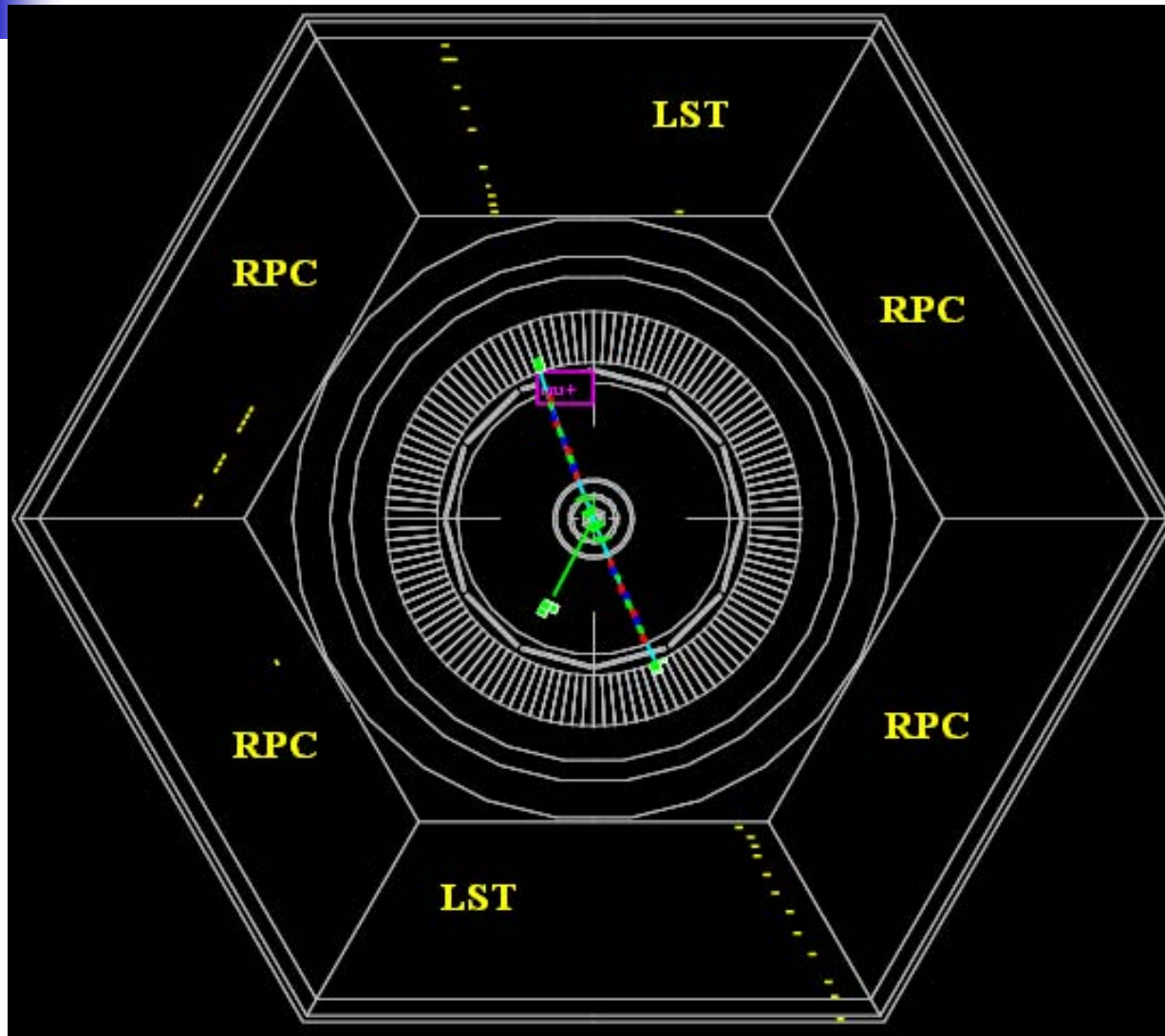
Proportional mode



Streamer mode



An event from the beam collision



Top and bottom sextants
are LSTs

Side four sextants are
RPCs

Online Detector Control (I)

IFR in BABAR main control panel

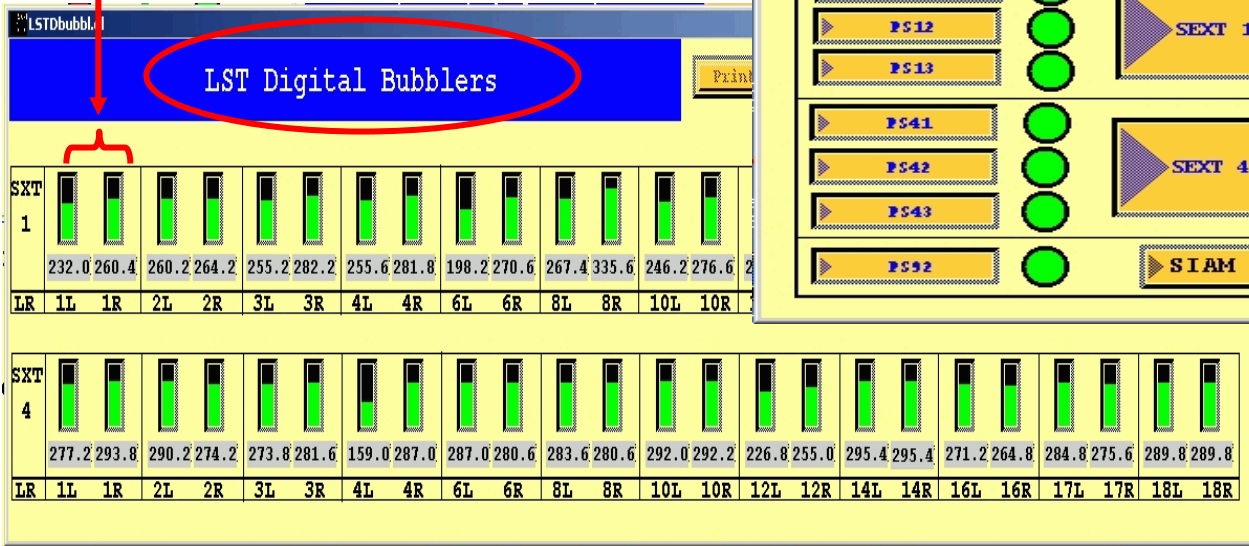
Separate subsystems
LST and RPC

Online Detector Control (II)

During injection of beam

During Physics run

Bubbler reading



Instrumented Flux Return LST Online Detector Control
Version 1.3

HV CONTROL
LOCAL
Off
Injectable
Runnable
GLOB_SET

LST status
HV FEE FEC GAS iocs ALL
LST is INJECTABLE
LST is RUNNABLE
HV FEE F1 B1 F4 B4

HV system
Power supplies ON Sextant view
PS11 PS12 PS13 PS41 PS42 PS43 PS92
SEXT 1 SEXT 4 SIAM

FEC crates
SUMMARY
Cr F1 Cr B1 Cr F4 Cr B4
FEE

Gas system
Gas GMB
Faults

Bubblers
DBUBBL

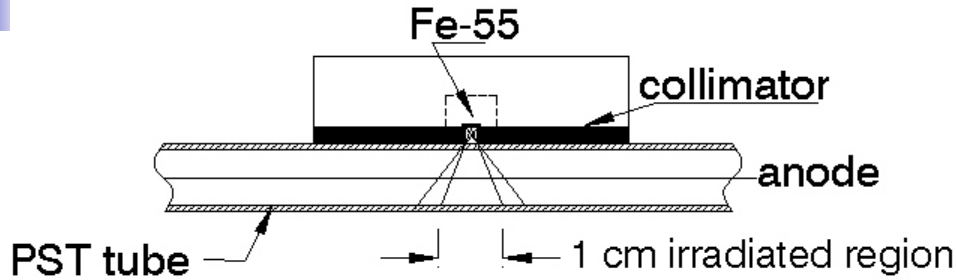
Humidity/temp
LST_HUM

IOCs
IER-IOM cr
IER-IV cr

Archiver
Ambient

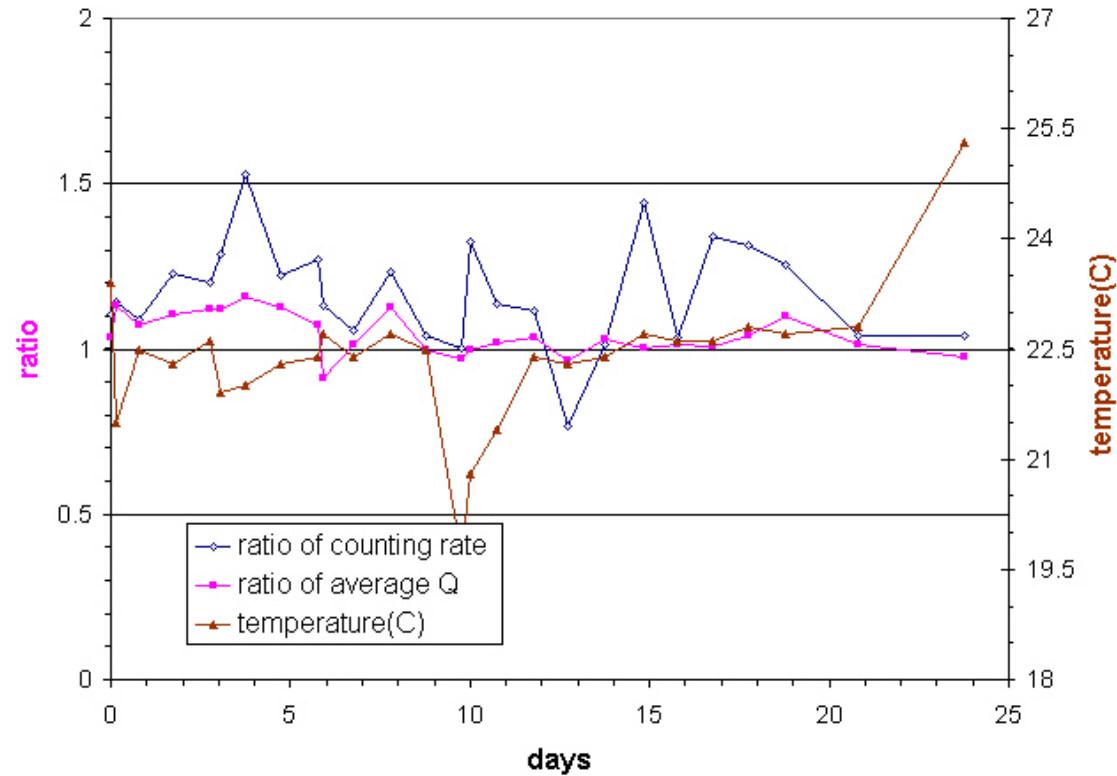
StripTool
Start ST

Aging test



X-ray irradiation distribution along anode wire direction

The ratio between the aging window and control window also shows no sign of aging.



Important Physics study using IFR detector (I)

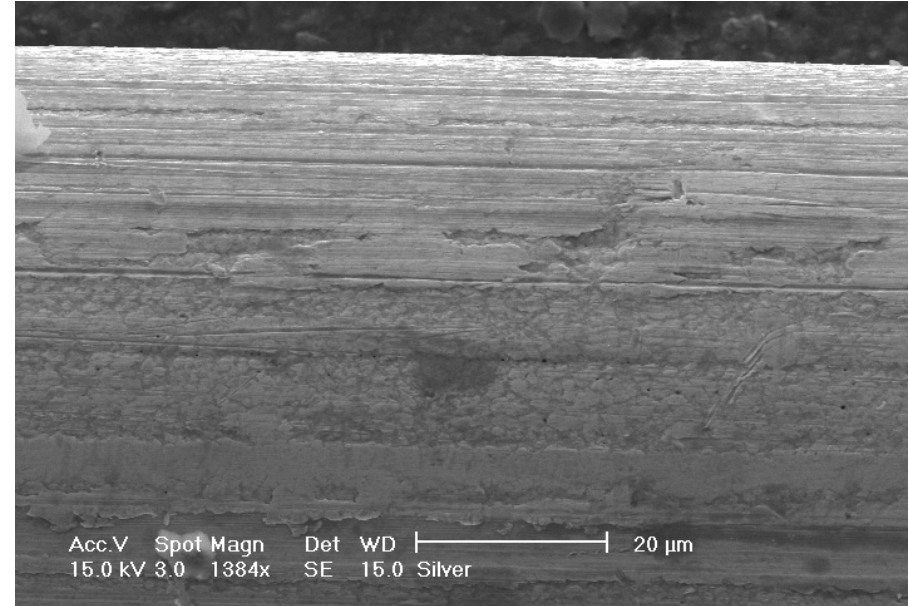
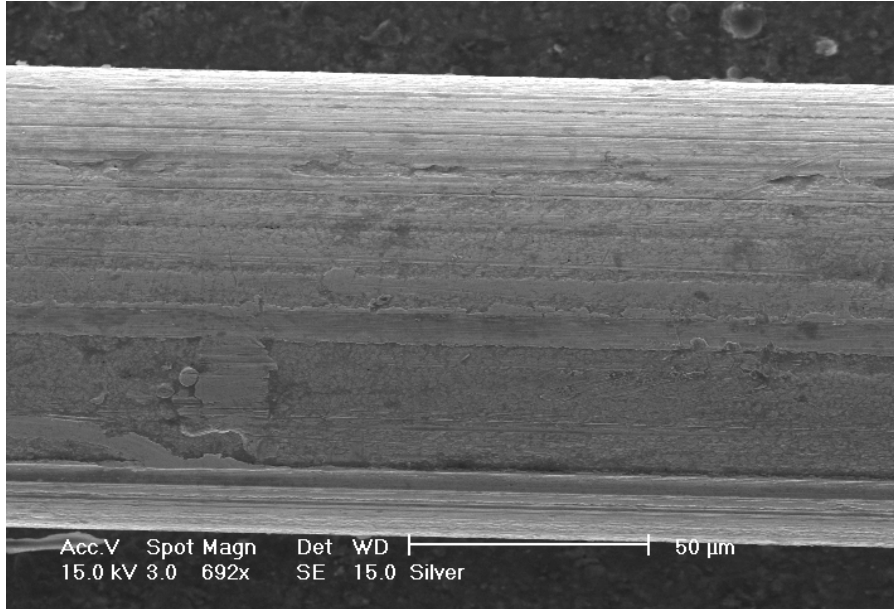
Process	Physics Goals	Role of muons	Role of K_L^0	Comments
$B \rightarrow \pi \ell^- \bar{\nu}, B \rightarrow \eta \ell^- \bar{\nu}, \dots$	BR, V_{ub} , dN/dq^2	***		stat, high p
$B \rightarrow \rho \ell^- \bar{\nu}, B \rightarrow \omega \ell^- \bar{\nu}, \dots$	BR, V_{ub} , dN/dq^2	***		stat, high p
$B \rightarrow X_u \ell^- \bar{\nu}$ (with B_{reco} sample)	BR, V_{ub}	***		stat, high p
$B \rightarrow X_u \ell^- \bar{\nu}$ (incl. endpoint)	BR, V_{ub}	***		high p
$B \rightarrow D \ell^- \bar{\nu}$	BR, V_{cb} , dN/dq^2	**		stat at high q^2
$B \rightarrow D^* \ell^- \bar{\nu}$	BR, V_{cb} , dN/dq^2	**		stat at high q^2
$B \rightarrow D_1 \ell^- \bar{\nu}, D_2^* \ell^- \bar{\nu}, D^{(*)} \pi \ell^- \bar{\nu}$	BR, V_{cb}	**		stat
$B \rightarrow X_c \ell^- \bar{\nu}$ (inclusive)	BR, V_{cb}	**		stat
$B \rightarrow X_c \ell^- \bar{\nu}$ (incl./ lepton tag)	BR, V_{cb}	**		stat
$B \rightarrow X_c \ell^- \bar{\nu}$ (mass moments)	BR, V_{cb}	**	* (?)	stat
$B \rightarrow D^{(*)} \tau^- \bar{\nu}$	BR, Higgs	**	* (?)	stat
$B \rightarrow K \ell^+ \ell^-$	BR, loops/new phys	****		stat
$B \rightarrow K^* \ell^+ \ell^-$	BR, loops/new phys	****		stat
$B \rightarrow X_s \ell^+ \ell^-$	BR, loops/new phys	***		stat
$B \rightarrow X_s \gamma$ (lepton tags)	BR, loops/new phys	**		stat
$B \rightarrow K \nu \bar{\nu}$	BR, loops/new phys		* (?)	stat

Rating system: IFR gives *(some benefit), ** (significant benefit),
 *** (large benefit), **** (essential information)

Modes highlighted in red will be discussed in more detail.

Silver plated anode wire

Images of Ag-plated Be-Cu wire



Surface quality looks similar to the Au-coated wire. Use SEM scale measured wire diameter is 107μm. Micrometer measured diameter is 105μm.

Both silver-plated and gold-plated Be-Cu wire samples look having smooth surface under the SEM.